Article

Climate Change Assessment in Brazil: Utilizing the Köppen-Geiger (1936) Climate Classification

Rafael Fausto de Lima[1] ⓘD, Lucas Eduardo de Oliveira Aparecido[2] ⓘD,
Guilherme Botega Torsoni[3] ⓘD, Glauco de Souza Rolim[1] ⓘD

[1]*Departamento de Engenharia e Ciências Exatas, Universidade Estadual Paulista "Júlio de Mesquita Filho", Jaboticabal, SP, Brazil.*
[2]*Departamento de Agrometeorologia, Instituto Federal do Sul de Minas, Muzambinho, MG, Brazil.*
[3]*Departamento de Agrometeorologia, Instituto Federal de Mato Grosso do Sul, Naviraí, MS, Brazil.*

Resumo

Análises e previsões climáticas indicam mudanças significativas nos elementos climáticos, principalmente na temperatura média global, e variações nos padrões de precipitação, que podem ter efeitos profundos nos ecossistemas e na agricultura. Este estudo tem como objetivo avaliar os impactos das mudanças climáticas no território brasileiro usando a classificação climática de Köppen-Geiger (1936). Foram analisados dados climáticos em 4.942 localidades, abrangendo municípios do Brasil, de 1989 a 2019. Esses dados foram obtidos da plataforma NASA/POWER e complementados com projeções mensais de temperatura e precipitação do modelo BCC-CSM1-1, parte do CMIP5 (Coupled Model Intercomparison Project Phase 5), em quatro cenários de emissões (RCP 2.6, RCP 4.5, RCP 6.0 e RCP 8.5) para os períodos de 2041-2060 e 2061-2080. Os resultados revelam um aumento de temperatura em todos os cenários, com o RCP 8.5 indicando o aumento mais significativo, atingindo 4,30 e 5,42 °C para os períodos de 2041-2060 e 2061-2080, respectivamente. Além disso, o mês menos chuvoso do ano apresenta valores de precipitação superiores a 60 mm, levando ao predomínio da tipologia de clima tropical "A" em 82,94% da avaliação climática atual. Em contrapartida, nos cenários de mudança climática, foram observadas reduções nas áreas com clima temperado típico "C" e expansões nas classes de clima árido "B" e tropical em comparação com o padrão climático atual. Notavelmente, a classe BSh tem uma prevalência de 6,09% e 8,16% para os períodos de 2041-2060 e 2061-2080, respectivamente. As mudanças climáticas observadas sinalizam possíveis desafios para a preservação de espécies no Brasil, pois as temperaturas mais altas podem dificultar sua adaptabilidade a condições mais secas e quentes. Como resultado, são necessárias medidas e estratégias cuidadosas para lidar com as implicações dessas mudanças nas próximas décadas.

Palavras-chave: projeções CMIP5, cenários de emissão, clima árido, temperatura média global.

Abstract

Analyses and climate forecasts indicate significant changes in climate elements, particularly the global mean temperature, and variations in rainfall patterns, which can have profound effects on ecosystems and agriculture. This study aims to assess the impacts of climate change on the Brazilian territory using the Köppen-Geiger (1936) climate classification. Climate data were analyzed at 4,942 locations, encompassing municipalities in Brazil from 1989 to 2019. These data were obtained from the NASA/POWER platform and complemented with monthly temperature and rainfall projections from the BCC-CSM1-1 model, part of the CMIP5 (Coupled Model Intercomparison Project Phase 5), under four emission scenarios (RCP 2.6, RCP 4.5, RCP 6.0, and RCP 8.5) for the periods 2041-2060 and 2061-2080. The findings reveal a temperature increase across all scenarios, with RCP 8.5 indicating the most significant rise, reaching 4.30 and 5.42 °C for the periods 2041-2060 and 2061-2080, respectively. Additionally, the least rainy month of the year exhibits precipitation values exceeding 60 mm, leading to the dominance of the tropical climate typology "A" in 82.94% of the current climate assessment. In contrast, under climate change scenarios, reductions in areas with typical temperate cli-

Correspoding author: Rafael Fausto de Lima. E-mail: rf.lima@unesp.br.

mate "C" and expansions in arid climate "B" and tropical climate classes were observed compared to the present climate pattern. Notably, the BSh class has a prevalence of 6.09% and 8.16% for the periods 2041-2060 and 2061-2080, respectively. The observed climate changes signal potential challenges for the preservation of species in Brazil, as higher temperatures may hinder their adaptability to drier and warmer conditions. As a result, careful measures and strategies are needed to address the implications of these changes in the coming decades.

1. Introduction

In summary, climate consists of climate elements observed in a given location (Rolim and Aparecido, 2016; Rigal *et al.*, 2019). The mean pattern of the atmosphere requires an analysis of time series with at least 30 years (WMO, 2017; Arguez *et al.*, 2012), achieving higher accuracy in the seasonal variation of climate elements (Teegavarapu *et al.*, 2012). Climate classification systems are important tools for assessing the mean scenarios in a region (Terassi and silveira, 2013), consisting of determining conditions for synthesizing and delimiting areas under similar conditions (Martins *et al.*, 2018), facilitating the comparison between climate variability of a particular location (Ayoade, 2010).

Several climate classification systems have been developed over time (Silva and Sales, 2018; Saifudeen *et al.*, 2023) considering climate factors or the effect of climate elements on physical and biological systems on Earth (Nascimento *et al.*, 2016; Netzel and Stepinski, 2016; Belda *et al.*, 2017). The most used systems are global wind zones and air masses of Flonh (1950) and Strahler (1951), vegetation cover of Candolle (1874), Köppen-Geiger (1936), Thornthwaite (1948), Holdridge (1967), and Camargo (1991). The Köppen system is the most used because of its accuracy (Rubel and Kottek, 2010; Alvarez *et al.*, 2013).

The Köppen system was based on the concept that native vegetation is the best expression of climate (De castro *et al.*, 2007; Tatli, 2017; Fernandez *et al.*, 2017), through the abundance and distribution of rainfall indices in the annual and monthly temperature variability (Medeiros *et al.*, 2020). The Köppen (1900) climate classification was developed through the relationship between vegetation using five vegetation groups (Ruman, 2020). Subsequently, the system underwent continuous changes performed by Köppen (1936), Setzer (1966), and Trewartha (1954), with higher importance in meteorology from Geiger (1961), making the system known as Köppen-Geiger (Rahimi *et al.*, 2020).

Climate change is one of the main threats to the ecosystems (Luis, 2015; Tamaki *et al.*, 2017; Pecl *et al.*, 2017; He and Silliman, 2019; Litke *et al.*, 2023), affecting aspects of human life and the environment (Rahimi *et al.*, 2020), with agricultural production being the most climate-dependent among all human activities (Adefisan, 2018). Several studies have assessed climate change around the world, for example, in Europe (Gallardo *et al.*, 2013), Serbia (MihailoviC *et al.*, 2015), Algeria (Zeroual *et al.*, 2019), and Australia (Leao, 2014), but none of them assessed Brazil using the Köppen-Geiger climate classification.

The use of climate classification systems as tools for validating climate change models (Belda *et al.*, 2014; Skalák *et al.*, 2018) represents an important subsidy tool to characterize new areas suitable or unsuitable for agricultural activity according to future climate change scenarios (Lori *et al.*, 2017; King *et al.*, 2018; Fathi and Ezziyyani, 2019).

The Intergovernmental Panel on Climate Change (IPCC) was created in 1988 by the World Meteorological Organization (WMO) and the United Nations Environment Program (UNEP) (IPCC, 2014) to provide assessments on climate change and its possible implications and future risks (Waisman *et al.*, 2019). According to IPCC (2012), climate change is the result of changes in climate, which are identified by changes in the mean and/or variability of its properties, with the value being maintained for a long period.

In the context of global warming, there is a gradual decrease in cold events while hot events are steadily increasing (Zhang and Gao, 2023). Simulation models project even greater changes for high-emission scenarios (Hamed *et al.*, 2023). The combined consequences of these phenomena are severe for rural regions, which could experience production losses with implications for food security (Straffelini and Tarolli, 2023), primarily due to water resource scarcity (Lehner and Formayer, 2023).

Climate reports generated by the IPCC are eventually issued to estimate these climate variations, showing emission scenarios based on changes in the greenhouse gas concentrations, rainfall levels, and variable thermal indices (IPCC, 2014). The fifth report of the IPCC (AR5) stated that the mean surface air temperature over land areas has increased by about 0.85 °C since 1880 (IPCC, 2013; O'neill *et al.*, 2016).

Representative concentration pathways (RCPs) are a set of four future climate change scenarios that form the basis for the Coupled Model Intercomparison Project Phase 5 (CMIP5) (Taylor *et al.*, 2012) and the assessment in the fifth report (AR5) issued by the IPCC (IPCC, 2013). CMIP5 represents the world's largest climate data project (Sanderson *et al.*, 2015). RCPs are mitigation scenarios that assume that political actions will be taken to achieve certain emission targets (Taylor *et al.*, 2012). RCPs present a scenario of lower greenhouse gas emissions (RCP2.6),

two intermediate scenarios (RCP4.5 and RCP6.0), and a scenario with very high emissions (RCP8.5) (IPCC, 2014).

The RCP 2.6 scenario shows a peak in radiative forcing of 3 W m^{-2} (~490 ppm CO_2eq) before 2100, followed by a decrease to 2.6 W m^{-2} in 2100. RCPs 4.5 and 6.0 show radiative forcing values of 4.5 W m^{-2} (~650 ppm CO_2eq) and 6.0 W m^{-2} (~850 ppm CO_2eq), respectively, both with stabilization after 2100, whereas RCP 8.5 demonstrates an increasing radiative forcing of 8.5 W m^{-2} (~1370 ppm CO_2eq) in 2100 (Van vuuren *et al.*, 2011).

This study aimed to complement existing climate research in Brazil by evaluating the potential effects of climate change projections from CMIP5. The reference used for this assessment was the Köppen-Geiger (1936) climate classification, and the analysis focused on the Representative Concentration Pathways (RCP) scenarios, specifically RCP 2.6, RCP 4.5, RCP 6.0, and RCP 8.5. The primary objectives were to investigate the impacts on rainfall and temperature, as well as the spatial distribution of Köppen-Geiger climate zones across the Brazilian territory under varying scenarios.

2. Material and Methods

2.1. Study area

The work was carried out in the Brazilian territory (Fig. 1) located in South America, corresponding to an area of 8,547,403.5 km2 (Rebouças, 2003; IBGE, 2011). Brazil has great economic prominence for the agribusiness sector, representing 37% of GDP (Gross Domestic Product) (Bruno, 2019) especially the production of grains (Soybean and Corn) and livestock in the Midwest region
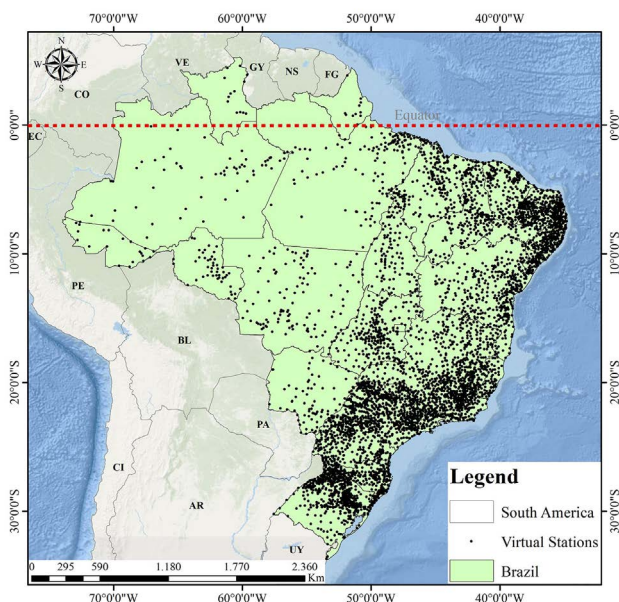

Figure 1 - Study area location map.

(Sauer and Leite, 2012). In Brazil, five biomes predominate: Amazon, Pantanal, Cerrado, Atlantic Forest and Pampas, providing different characteristics for the vegetation (Coutinho, 2016).

2.2. Database

The current scenario was calculated with climate data for temperature (°C) and precipitation (mm) obtained from the National Aeronautics and Space Administration/ Prediction of Worldwide Energy Resources - NASA/ POWER platform (Sparks, 2018) in the period 1989 - 2019 for 4942 municipalities distributed over the Brazilian territory (Fig. 1).

Using the geographic information system (GIS), the spatial interpolation of all climatic elements for the current scenario was performed using the Kriging method (Krige, 1951), with a spherical model, a neighbor and a spatial resolution of 0.25 °.

We used to evaluate climate change scenarios, data from monthly projections of temperature and precipitation extracted from the BCC-CSM1-1 model (Xiao-ge *et al.*, 2013), available on the CHELSA V1.2 platform (Climatologies at high resolution) were used. for the earth's land surface areas - https://chelsa-climate.org) (Karger, 2017). The model belonging to phase 5 of the CMIP corresponding to the years 2041-2060 and 2061-2080, associated with four RCP scenarios (2.6, 4.5, 6.0, 8.5).

The BCC-CSM1-1 model was developed by the Beijing Climate Center (BCC) (Xin *et al.*, 2018), it is a model of a coupled climate system including atmosphere, ocean, land surface and sea ice (Wu *et al.*, 2013).). The model is run on the National Center for Atmospheric Research (NCAR) coupler version 5 (Xiao-ge *et al.*, 2013).

2.3. Calculation of potential evapotranspiration

The calculation of potential evapotranspiration (*PET*) was performed using the method of Camargo (1971) using Eq. (1).

$$PET = F \ Qo \ T \ ND \qquad (1)$$

where *Qo* (mm day^{-1}) is the daily extraterrestrial solar radiation expressed in evaporation equivalent, in the considered period, *T* (°C) is the average air temperature during the period; *F* is the adjustment factor that varies with the average annual temperature (*Ta*) of the site (for *Ta* up to 23 °C, *F* = 0.01; *Ta* = 24 °C, *F* = 0.0105; *Ta* = 25 °C, *F* = 0.011; *Ta* = 26 °C, *F* = 0.0115; *Ta* > 26 °C, *F* = 0.012); and *ND* is the number of days in the period.

2.4. Climatological water balance

For the purpose of climatological characterization of current and future climate conditions, the climatic water balance (CWB) was employed. This method was based on
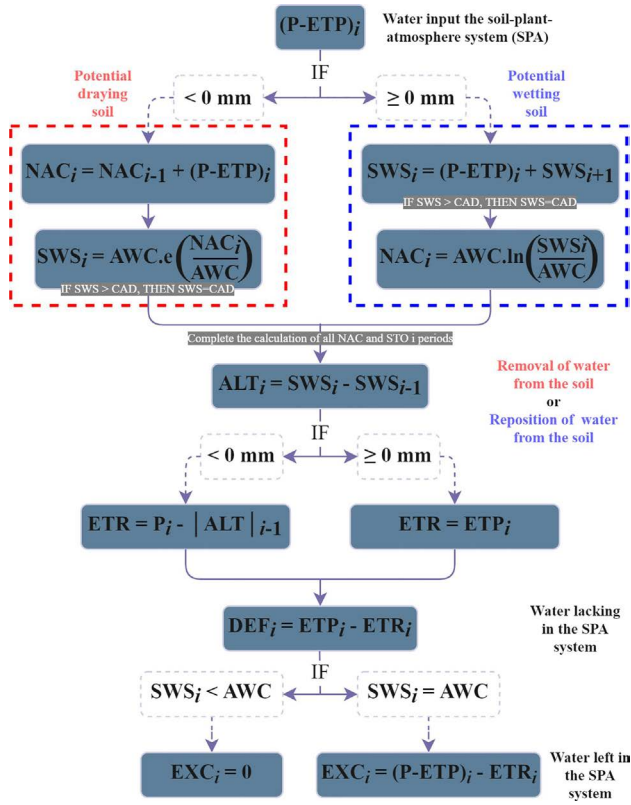
Figure 2 - Diagram of the modified water balance model by Thornthwaite and Mather (1955). where *PET* is the potential evapotranspiration (mm), *AWC* is the available water capacity in the soil (mm), *SWS* is the soil water storage (mm), *NAC* is the accumulated negative, i.e., accumulated precipitation minus potential evapotranspiration, *P* is the precipitation (mm), *DEF* is the water deficit in the soil-plant-atmosphere system (mm), *ETR* is the real evapotranspiration (mm), *EXC* is the water surplus of the soil-plant-atmosphere system (mm), *ALT* is the soil water storage for the current month minus soil water storage for the previous month (mm), and *i* is the monthly period. Adaptado de Rolim *et al.*, 2020.

the approach proposed by Thornthwaite and Mather (1955) (Fig. 2). A soil available water capacity of 100 mm was utilized, as it was found to be more suitable for regional climate characterization (De carvalho *et al.*, 2010; Rodrigues *et al.*, 2018).

2.5. Köppen-Geiger climate classification

The classification proposed by Köppen-Geiger uses a system composed of 3 letters to define climatic zones. Seeking to indicate the vegetation group based on temperature and precipitation values (first letter), annual precipitation distribution (second letter) and seasonal temperature variations (third letter) (Rahimi *et al.*, 2020), depending on the seasonality of temperature or precipitation (Köppen 1936; Geiger 1961).

The climatic classification was carried out using the Köppen-Geiger method (1936), following the descriptions

made by Peel *et al.* (2007), Kriticos *et al.* (2012), and Beck *et al.* (2018) (Fig. 3).

The system is identical to that adopted by Köppen (1936) with some differences, where the climates and cold "D" and temperate "C" are delimited using a limit of 0 °C for the coldest month. The arid subclimates "B" W (desert) and S (steppe) were identified, corresponding to 70% of the precipitation in summer or winter, and the subclimates s (dry summer), w (dry winter) and f (no dry season) within the C and D climates were made mutually exclusive, tropical "A", temperate "C", cold "D" and polar "E" climates can intersect with arid class "B", to avoid this, climate type B had preference over other classes. Seeking to normalize the temperature and precipitation indices during the seasons, summer and winter were defined as the period of six hottest and coldest months between October to March and April to September.

2.6. Statistical indicators

The climate data collected from the virtual stations (NASA/POWER) and the data estimated by the BCC-CSM1-1 model for the climate change scenarios were compared using statistical indicators: precision and accuracy (Table 1). Precision, indicating the degree of dispersion between estimated and observed values, was estimated by the coefficient of determination (R^2) as described by Cornell and Berger (1987). The accuracy, which determines the distance between estimated and observed values, was estimated using the Willmott index (*d*), mean square error (RMSE) and mean absolute error (MAPE).

3. Results and Discussion

The mean rainfall for Brazil was 1987 (± 725) mm (Fig. 4A), corroborating the values found by Casaroli *et al.*

Table 1 - Precision and accuracy of the statistical indices used. Where *Yesti* is the estimated value of y; *Yobsi* is the observed value of; $\overline{Y}$ is the observed mean value of y; *N* is data number.

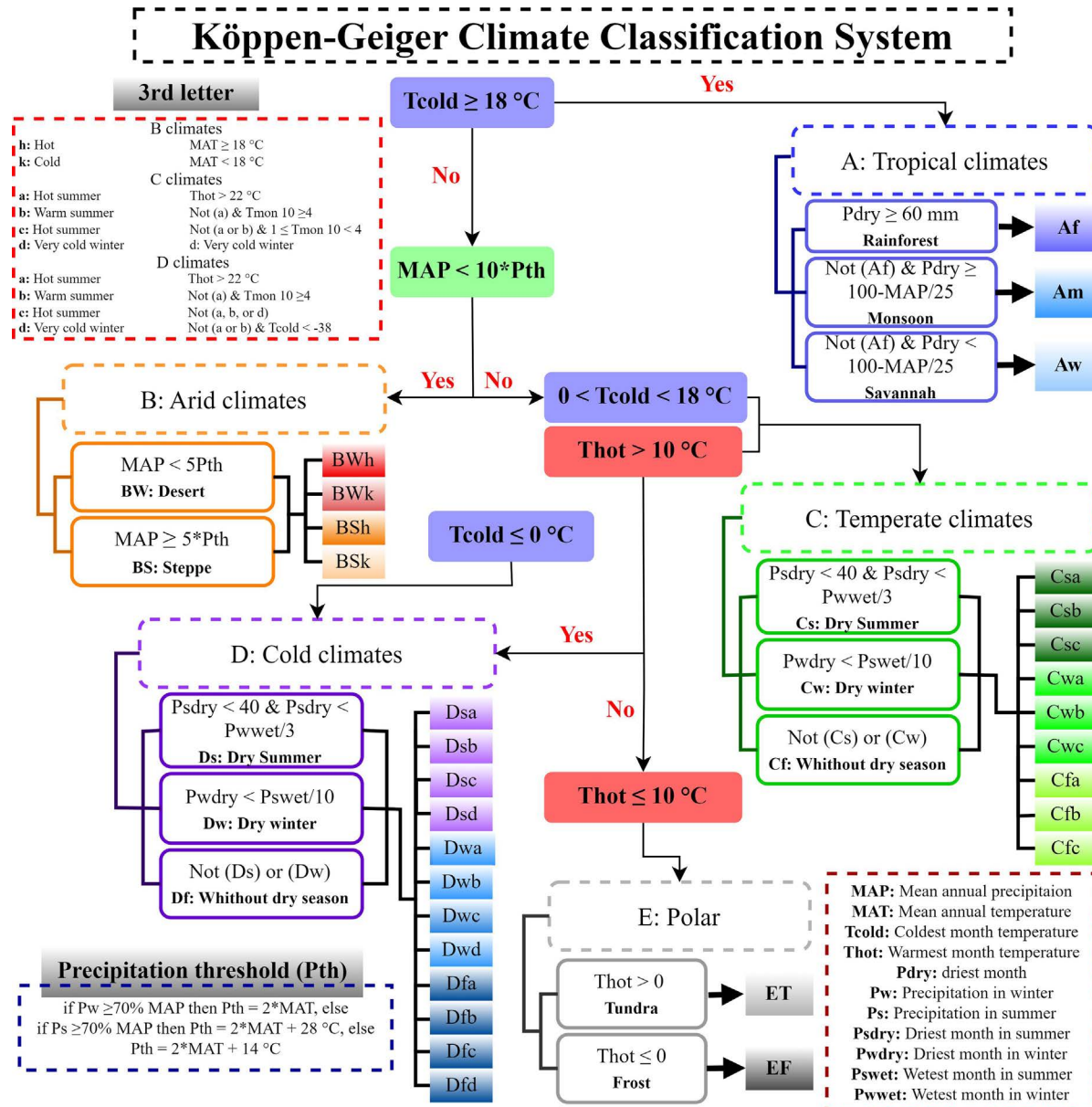| Statistical index	Equation
Precision	
R^2	$R^2 = 1 - \dfrac{\sum_{i=1}^{n}\left(Yesti - \overline{Y}obs\right)^2}{\sum_{i=1}^{n}\left(Yesti - \overline{Y}obs\right)^2 - \sum_{i=1}^{n}\left(Yesti - Yobsi\right)^2}$
Accuracy	
d	$d = 1 - \dfrac{\sum_{i=1}^{n}\left(Yobsi - Yesti\right)^2}{\sum_{i=1}^{n}\left(\left\lvert Yesti - \overline{Y}\right\rvert + \left\lvert Yobsi - \overline{Y}\right\rvert\right)^2}$
RMSE	$RMSE = \sqrt{\dfrac{\sum_{i=1}^{n}\left(Yobsi - Yesti\right)^2}{N}}$
MAPE	$MAPE = \dfrac{\sum_{i=1}^{n}\left(\frac{\lvert Yobsi - Yest\rvert}{Yobsi}\right)}{N} * 100$

Figure 3 - Köppen-Geiger climate classification flowchart.

(2018). However, variations from 409 to 3625 mm were found between regions. The states of Rio Grande do Norte and Amapá presented the lowest and highest mean annual rainfall, with values of 800.86 (± 213.18) and 2999.79 (± 305.32) mm, respectively. Similar results were observed by Almeida *et al.* (2017) and Gonçalves and Back (2018) on rainfall variability in Brazil. Air temperature for Brazil presented a mean of 22.20 (± 3.20) °C (Fig. 4B). Amapá and Santa Catarina showed the highest and lowest means of air temperature, with values of 27.10 (± 0.46) and 18.02 (± 1.51) °C, similar to what was reported by Medeiros *et al.* (2005) and Alvares *et al.* (2013a).

The statistical precision test reveals a higher dispersion between the mean annual temperature data for the periods 2041-2060 (Table 2) and 2061-2080 (Table 3). The period 2041-2060 shows an R^2 dispersion analysis of 0.64 and 0.58 for RCP 4.5 and 8.5, respectively, while the Willmott agreement index (d) remained below 0.50 for all RCPs. This dispersion coincides with the mean temperature rise projected by the scenarios. RMSE and MAPE for the RCP 8.5 scenario reached values of 4.50 and 19.97%, respectively. The following period (2061-2080) (Table 3) registered little difference relative to the previous period, showing a higher dispersion for RCP 8.5, with RSME of 25.04% and R^2 of 0.44.

The mean annual rainfall presents a lower dispersion between the observed data and the stipulated for the periods 2041-2060 (Table 2) and 2061-2080 (Table 3). The R^2
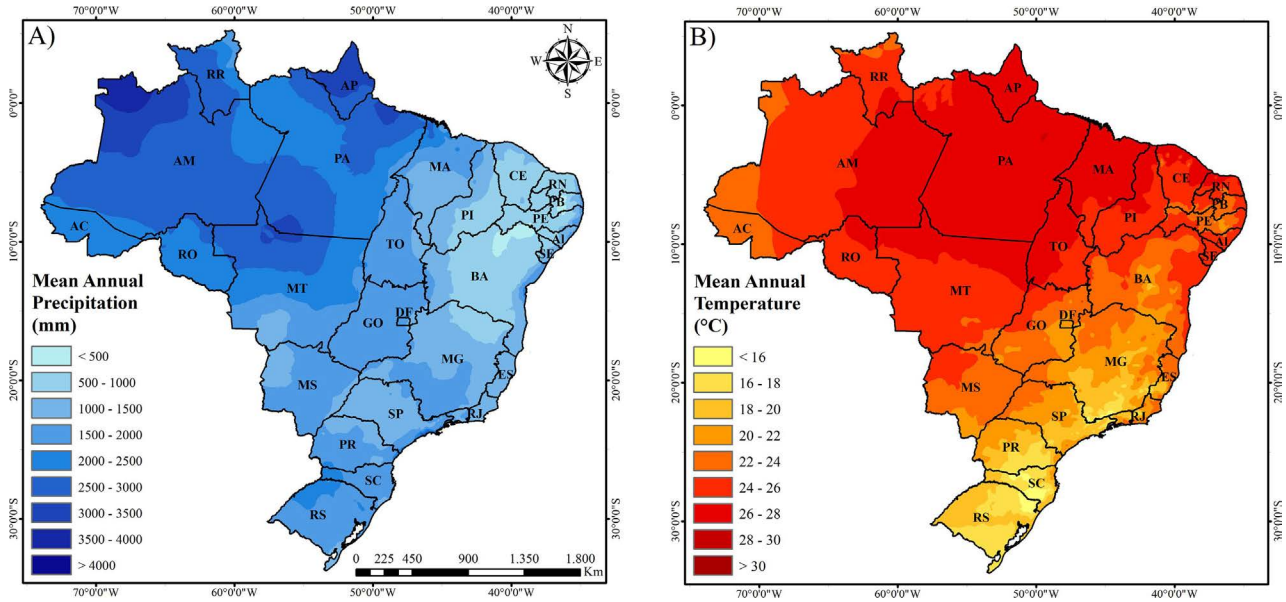
Figure 4 - Rainfall and temperature for current climate conditions from 1989 to 2019.

Table 2 - Statistical analysis for the period 2041-2060.

Statistical index	2041-2060							
	Mean annual temperature				Mean annual precipitation			
	RCP_2.6	RCP_4.5	RCP_6.0	RCP_8.5	RCP_2.6	RCP_4.5	RCP_6.0	RCP_8.5
R^2	0,68	0,64	0,74	0,58	0,96	0,97	0,98	0,93
d	0,49	0,45	0,47	0,42	0,88	0,91	0,93	0,88
RMSE	3,55	4,06	3,88	4,50	41,31	35,03	29,70	39,93
MAPE	15,54	17,93	17,16	19,97	22,51	19,84	17,81	25,24

Table 3 - Statistical analysis for the period 2061-2080.

Statistical index	2061-2080							
	Mean annual temperature				Mean annual precipitation			
	RCP_2.6	RCP_4.5	RCP_6.0	RCP_8.5	RCP_2.6	RCP_4.5	RCP_6.0	RCP_8.5
R^2	0,79	0,56	0,73	0,44	0,91	0,94	0,98	0,92
d	0,52	0,44	0,43	0,37	0,87	0,89	0,91	0,90
RMSE	3,32	4,20	4,34	5,59	42,24	38,73	33,22	37,33
MAPE	14,65	18,51	19,27	25,04	23,04	24,25	21,67	22,69

dispersion analysis remained above 0.90 for all assessed scenarios and the d index presented values close to 1, indicating little variation between the mean annual rainfall estimated by the model and that observed. RCP 2.6 for the period 2041-2060 presented the highest RSME, with a value of 41.31, and the RCP 8.5 scenario showed the highest MAPE, with a value of 25.24%, indicating higher data segregation. In the period from 2061 to 2080, the RCP 6.0 scenario presented lower RSME and MAPE indices, reaching values of 33.22 and 21.97, respectively.

Rainfalls under climate change scenarios in the period 2041-2060 showed a decrease in the mean annual volume for Brazil, ranging from -159 to -255 mm (Fig. 5). In general, the spatial rainfall distribution between scenarios showed no variation. However, it evidenced an increase mainly in the west of the state of Amazonas, in the north of Pará, and the entire Amapá, while the northeast region of Brazil had the lowest values of annual rainfall. The highest difference between scenarios was observed for the annual rainfall volume.
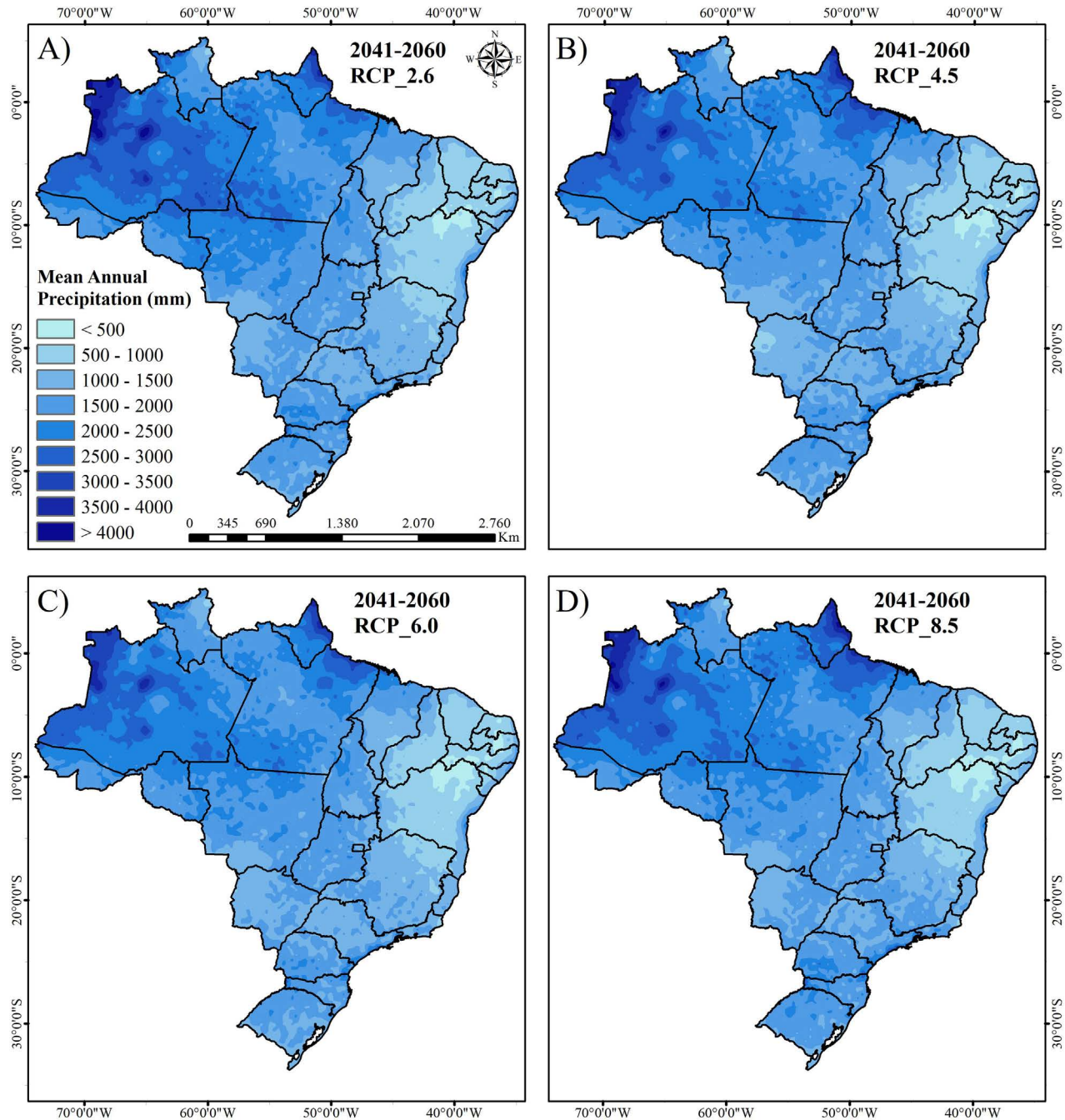
Figure 5 - Mean annual rainfall for climate change scenarios in the period 2041-2061.

RCP 2.6 showed an annual mean of 1827 (± 677) mm, being the scenario with the highest rainfall volume. RCP 8.5 showed the second-highest volume, with an annual mean of 1808 (± 657) mm. RCP 6.0, on the other hand, had the lowest rainfall among all scenarios, with a value of 1731 (± 603) mm per year. Moreover, RCP 4.5 presented a mean of 1772 (± 637) mm. The observed data were similar to those assessed by Dabanli (2018) when analyzing the relationship of the difference between tem-

perature and rainfall under climate change scenarios in Turkey.

A percentage rainfall variation of -60% to +60% is observed relative to the different scenarios (Fig. 6). However, predominant variations of 0-30% are observed in a large part of the Brazilian territory. The largest reductions in rainwater supply were between the states of Roraima, extreme north of Amazonas, Mato Grosso and Bahia, west of Rondônia, Acre and Mato Grosso do Sul, the center of
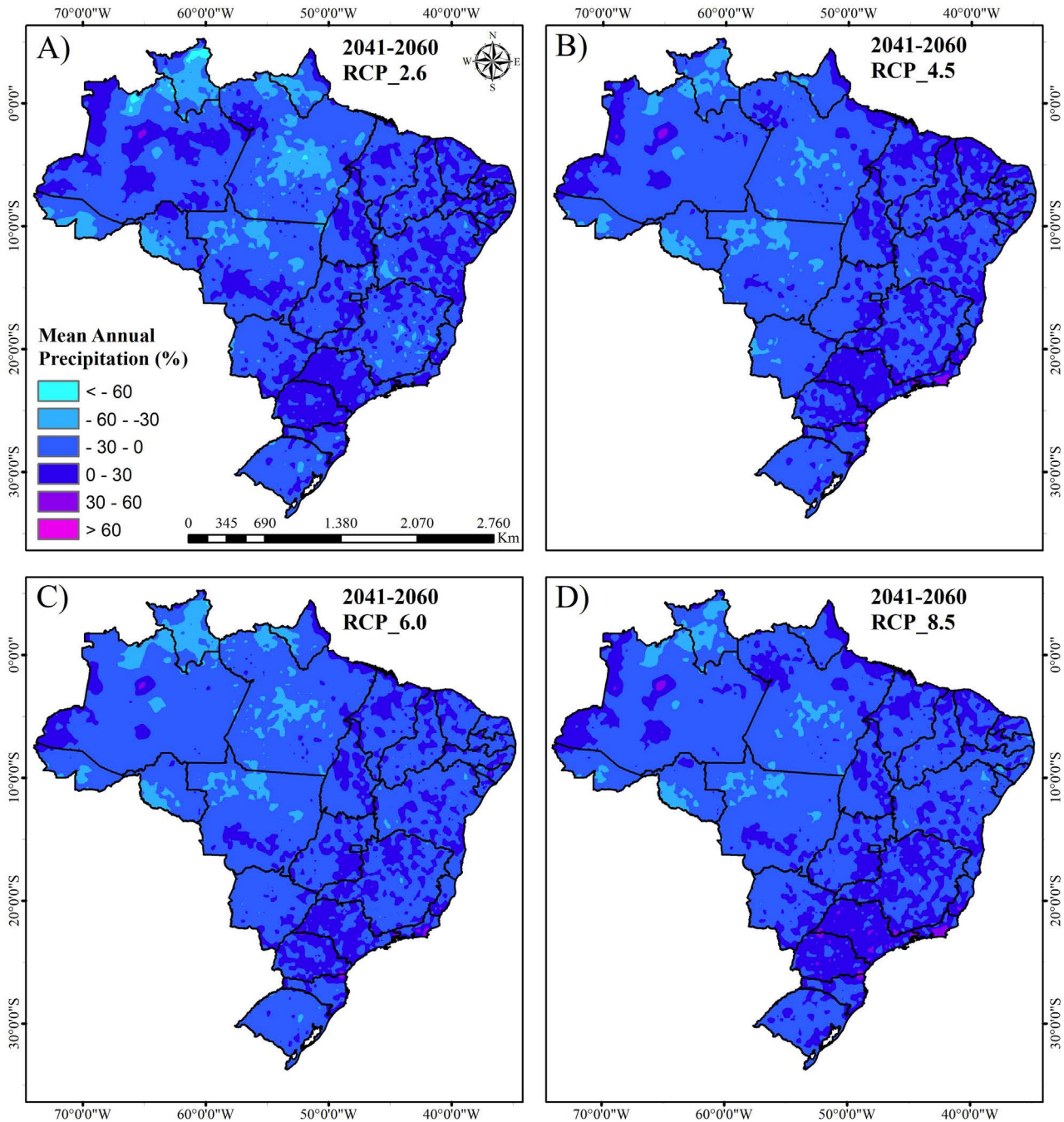
Figure 6 - Dynamics of mean annual rainfall for climate change scenarios during the period 2041-2060.

the state of Pará, and small areas dispersed throughout the state of Minas Gerais, with values ranging from 30 to 60%. On the other hand, an increase of up to 60% is observed in the west of Amazonas, the coastline of Rio de Janeiro, and small locations of the north and coastline of Paraná.

A high variation of the mean air temperature was observed in the 2041-2060 scenarios relative to the current scenario, varying 3.6 ($\pm$ 0.49) °C on average (Fig. 7). RCP 2.6 showed the lowest variation compared to the current

scenario, with an annual mean of 25.54 ($\pm$ 2.28) °C, concentrated in the North and Northeast regions (Fig. 7A). Conversely, RCP 8.5 reached 26.54 ($\pm$ 2.40) °C, with the highest variation compared to the current scenario (Fig. 7D).

The RCP 4.5 scenario showed the second-highest annual mean of air temperature, with a value of 26.06 ($\pm$ 2.30) °C (Fig. 5B), exceeding the mean of the RCP 6.0 scenario, which presented a value of 25.90 ($\pm$ 2.31) °C (Fig. 7C). Miao *et al.* (2014) also observed a similar dif-
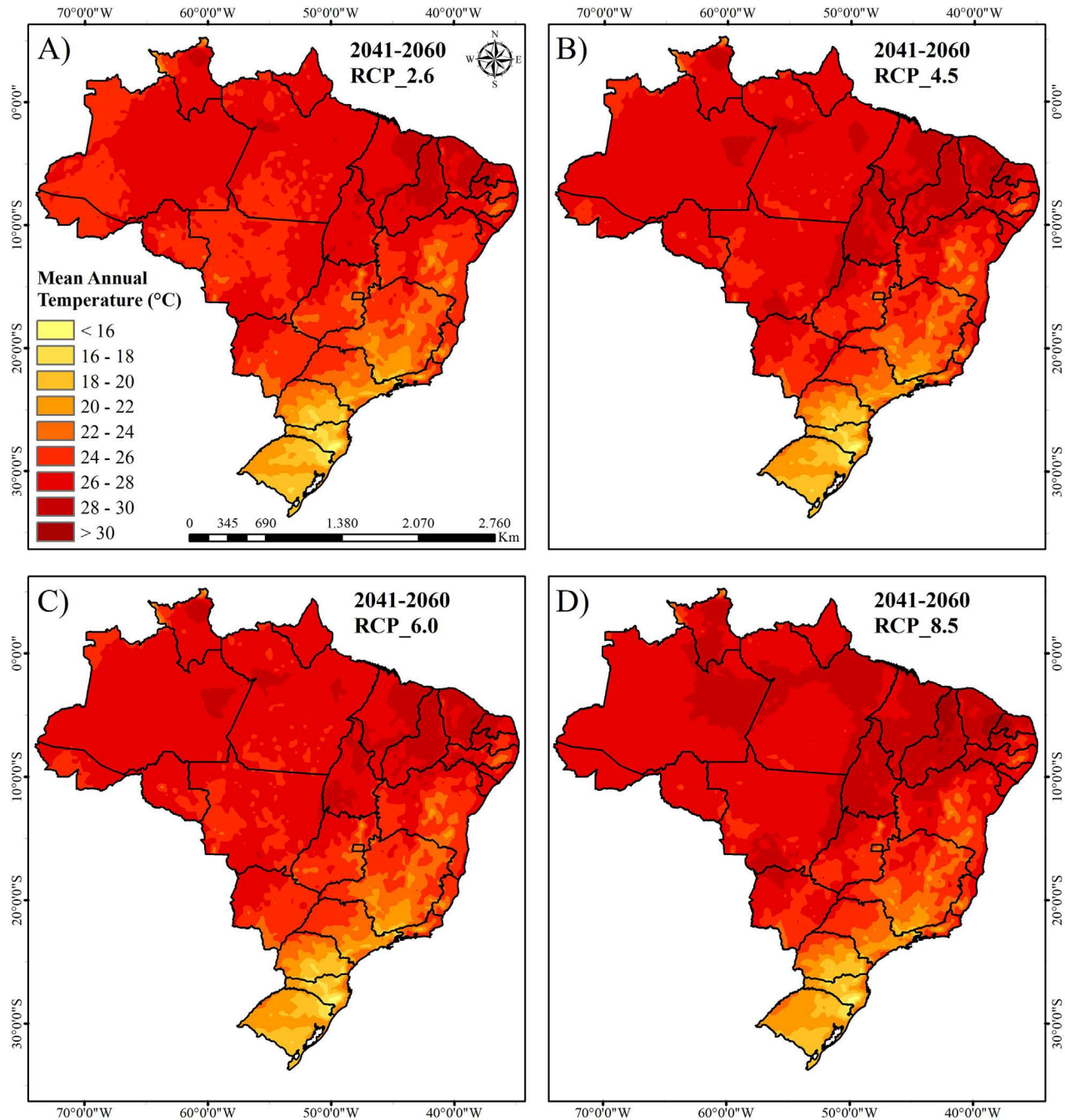
Figure 7 - Mean annual temperature for climate change scenarios in the period 2041-2060.

ference when assessing CMIP5 climate models and projecting temperature changes in Northern Eurasia.

Reductions in the mean temperature of -10% can be found in the states of Pará, Amapá, northern Mato Grosso and Maranhão, eastern Rondônia, and southern Amazonas for RCPs 2.6, 4.5, and 6.0 (Figs. 8A, B, and C). An increase in temperature of more than 20% was observed in small points in western São Paulo and Minas Gerais, Rio de Janeiro, and Espírito Santo for RCP 2.6 (Fig. 8A). In

the other scenarios, this increase can also be observed in the north of Roraima for RCP 4.6 and 6.0 (Figs. 8B and C) and a few places in the states of Bahia, Piauí, Paraíba, and Ceará for RCP 8.5 (Fig. 8D).

The scenarios of the period 2061-2080 showed rainfall with a small reduction relative to the previous period, with values of 3.64 mm. The mean observed between scenarios reached 1781.24 (± 41.18) mm per year (Fig. 9). The spatial distribution of rainfall showed
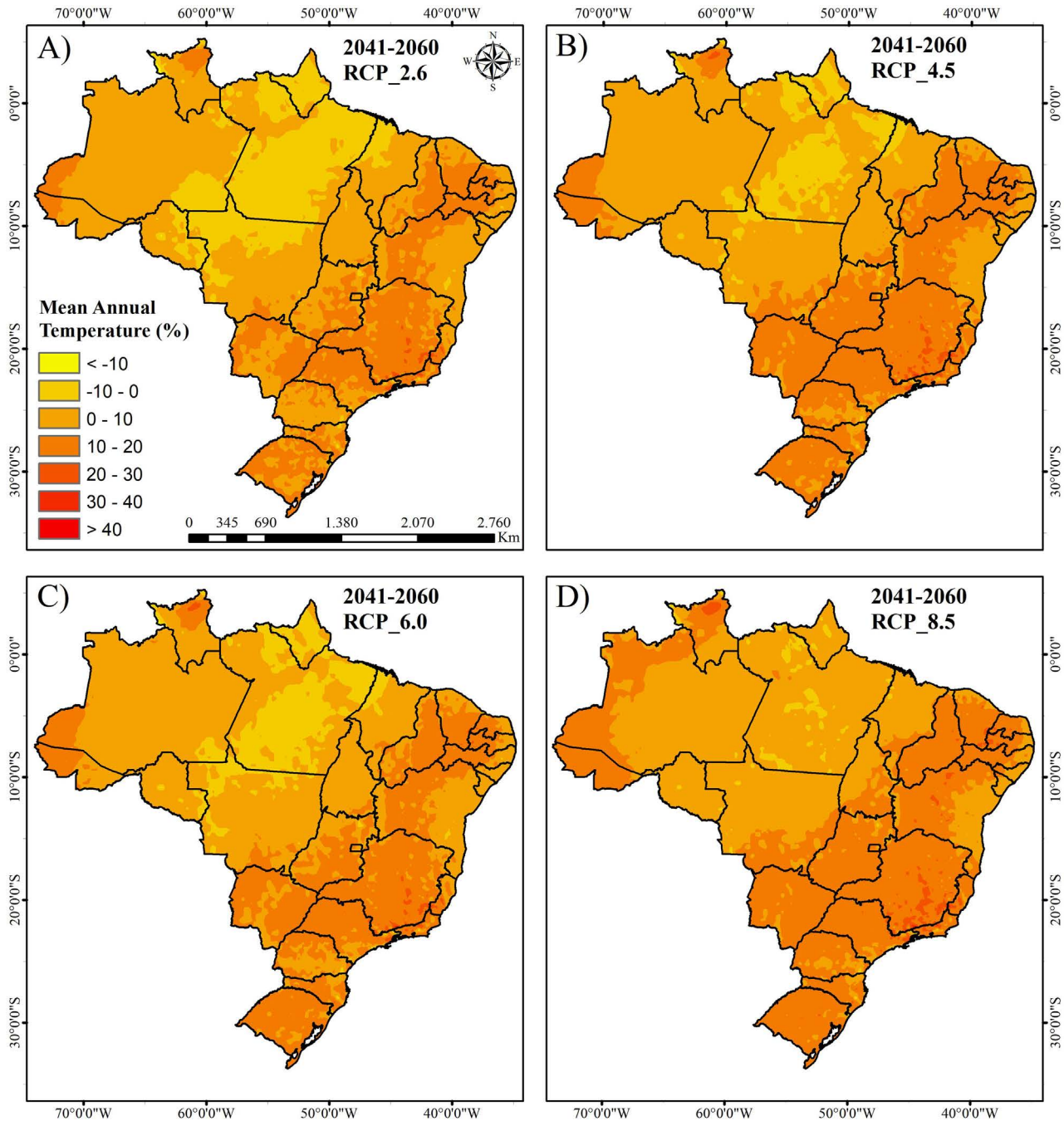
Figure 8 - Mean annual temperature variation for climate change scenarios in the period 2041-2060.

no change relative to the period 2041-2060, with the North region having the highest rainfall volumes. RCP 2.6 presented a mean of 1835 (± 638) mm (Fig. 9A), being the scenario with the highest volume. The RCP 8.5 scenario had the lowest rainfall volume, with a mean of 1741 (± 644) mm (Fig. 9D). RCP 4.5 and 6.0 had annual means of 1790 (± 659) and 1750 (± 635) mm (Figs. 9B and C).

Rainfall variation for RCP 2.6 and 4.5 (Figs. 10A and B) remained equal to the previous period. RCP 6.0

and 8.5 showed reductions in rainfall of up to -60%, with higher intensity in the states of Pará, Roraima, and Amapá and also in the entire Northeast region (Fig. 10).

Air temperature for the scenarios in the period 2061-2080 showed an increase compared to the period 2041-2060 (Fig. 11). RCP 8.5 (Fig. 11D) showed the highest increase compared to the previous period (1.12 °C), with an annual mean of 27.62 (± 2.42) °C, being the scenario with the highest mean temperature. This increase can negatively influence agricultural production in the region
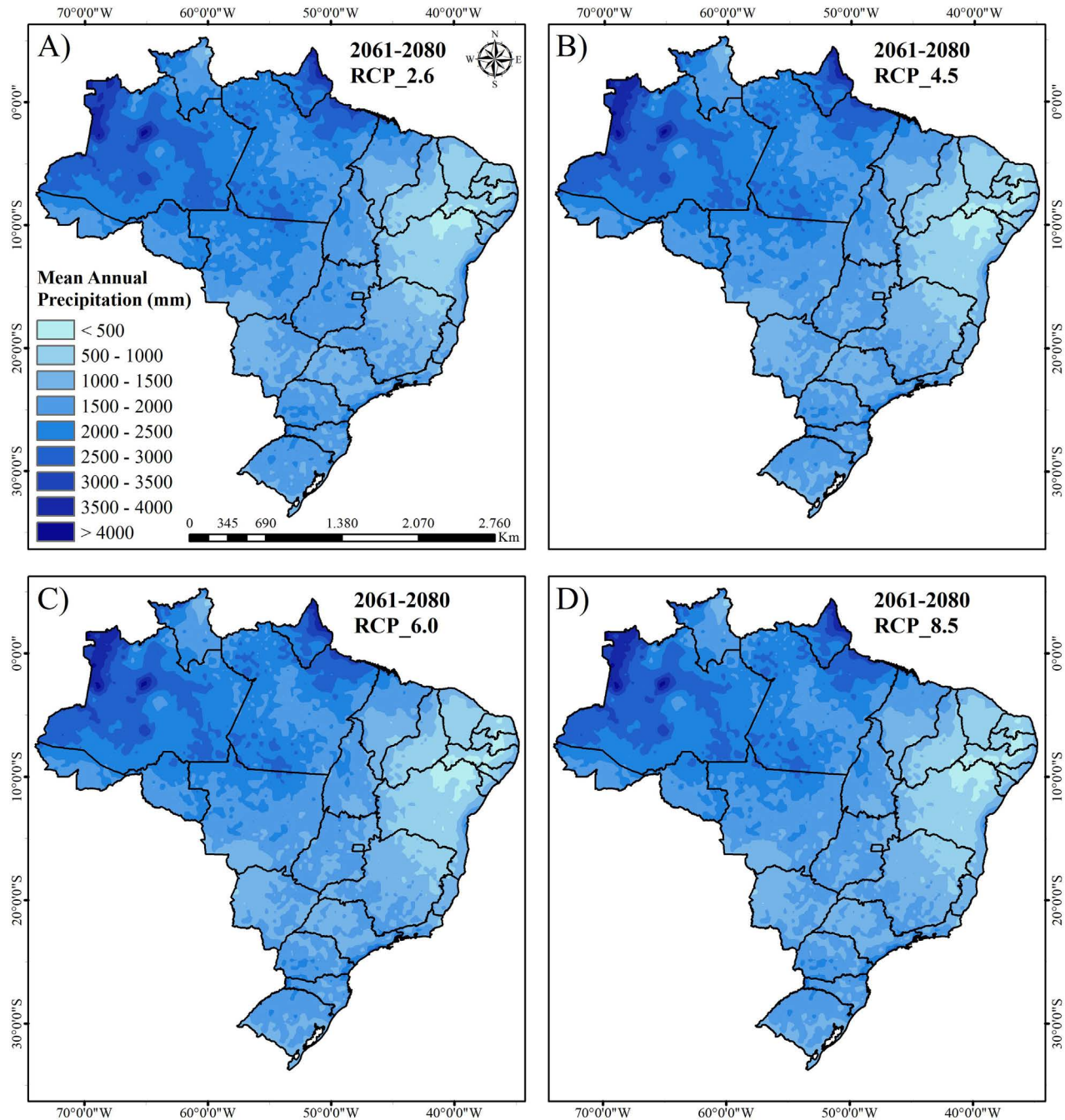
Figure 9 - Mean annual rainfall for climate change scenarios in the period 2061-2080.

due to the large temperature variation (Srivastava *et al.*, 2018).

The RCP 2.6 scenario (Fig. 11A) showed a small reduction in temperature compared to the previous period, with an annual mean of 25.36 (± 2.29) °C, characterizing the scenario with the lowest mean air temperature during this period. RCP 4.5 and 6.0 (Figs. 11B and C) showed similar means of air temperature, with values of 26.19 (± 2.35) and 26.35 (± 2.31) °C, respectively.

A 10% reduction was observed in the mean annual temperature, with a predominance in the same locations highlighted for the previous period in RCP 2.6, 4.5, and 6.0 (Figs. 12A, B, and C), except for RCP 8.5, showing an increase in temperature. An increase of more than 20% in the mean temperature occurred at small points in the west of São Paulo and Minas Gerais, Rio de Janeiro, Espírito Santo, and Amapá for RCP 2.6 and 4.5 (Figs. 12A and B) and few locations in the states of
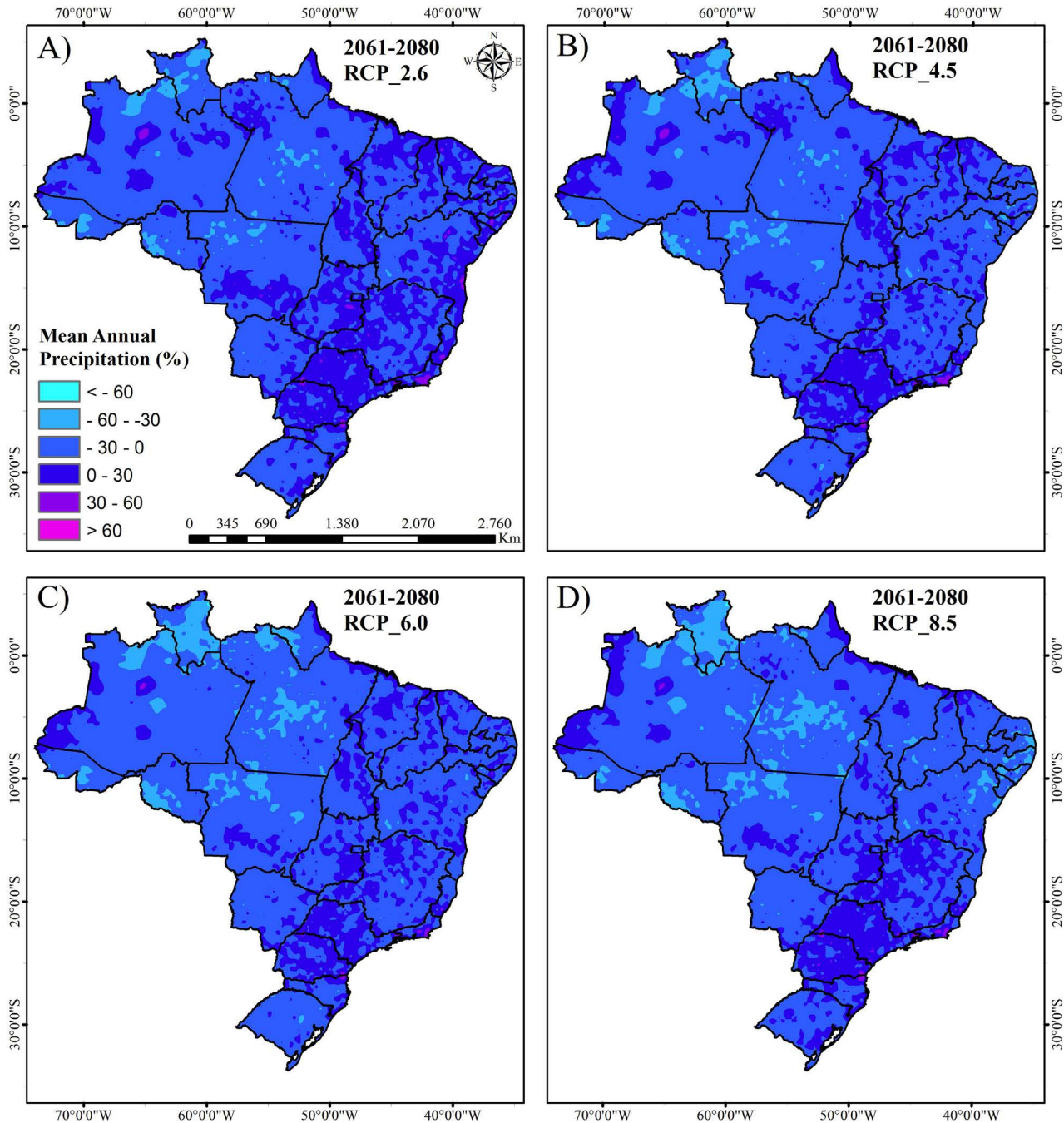
Figure 10 - Mean annual rainfall variation for climate change scenarios in the period 2061-2080.

Bahia, Piauí, Paraíba, and Ceará for RCP 6.0 (Fig. 12C). The states of the South, Southeast, Northeast, and Midwest regions of Brazil and the west of Acre and Amazonas showed a 20% increase in the mean temperature for RCP 8.5 (Fig. 12D).

The analysis of the vulnerability of Brazilian states to changes in rainfall patterns and mean air temperature showed that the state of Paraná (Fig. 13PR) had the highest increase in rainfall, with increments of +200 (1788 ± 41) mm, +69 (1657 ± 40) mm, +92 (1680 ± 39) mm, and +217 (1805 ± 55) mm for RCPs 2.6, 4.5, 6.0, and 8.5, respectively, in the period 2041-2060. The Federal District (Fig. 13DF) represents the second most favorable location for increased rainfall in Brazil, with an increase of +148 mm for RCPs 2.6 (1680 ± 116) mm, 4.5 (1680 ± 120) mm, 6.0 (1746 ± 118) mm, and 8.5 (1745 ± 118) mm.

Roraima (Fig. 13RR), Amapá (Fig. 13AP), and Rondônia (Fig. 13RO) represent the states with the highest reduction in rainfall for the period 2041-2060. The state of
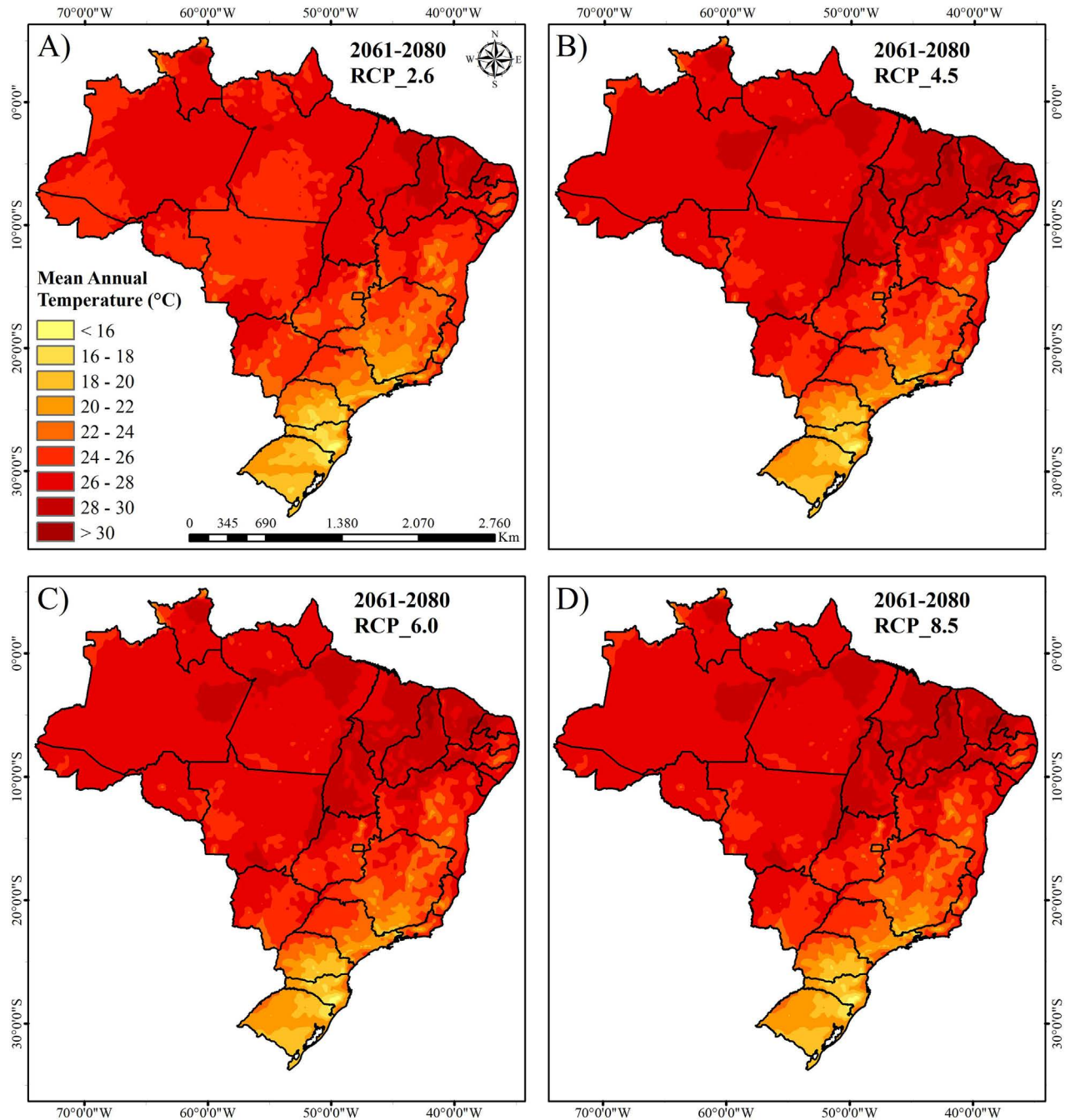
Figure 11 - Mean annual temperature for climate change scenarios in the period 2061-2080.

Roraima presented reductions of -725 (1589 ± 91) mm, -753 (1562 ± 88) mm, -853 (1462 ± 84) mm, and -723 (1592 ± 101) mm for RCPs 2.6, 4.5, 6.0, and 8.5 respectively, being the Brazilian state with the highest reduction for the period 2041-2060. The state of Amapá had RCPs 2.6 and 6.0 with the highest levels of reduction in rainfall, with values of -579 (2420 ± 132) mm and -541 (2458 ± 139) mm, respectively. The state of Rondônia showed reductions of -304 (2072 ± 128) mm, -531 (1845 ±

104) mm, -475 (1901 ± 114) mm, and -463 (1913 ± 111) for RCPs 2.6, 4.5, 6.0, and 8.5 respectively.

All 26 states and the Federal District showed an increase in the mean annual temperature in the assessed scenarios for the period 2041-2060 (Fig. 14), especially the Federal District (Fig. 14DF), location with the highest increase in temperature, with values of +3.92 (24.90 ± 1.20) °C, 4.62 (25.60 ± 1.29) °C, 4.17 (25.15 ± 1.14) °C, and 4.92 (25.90 ± 1.28) °C for RCPs 2.6, 4.5, 6.0, and 8.5,
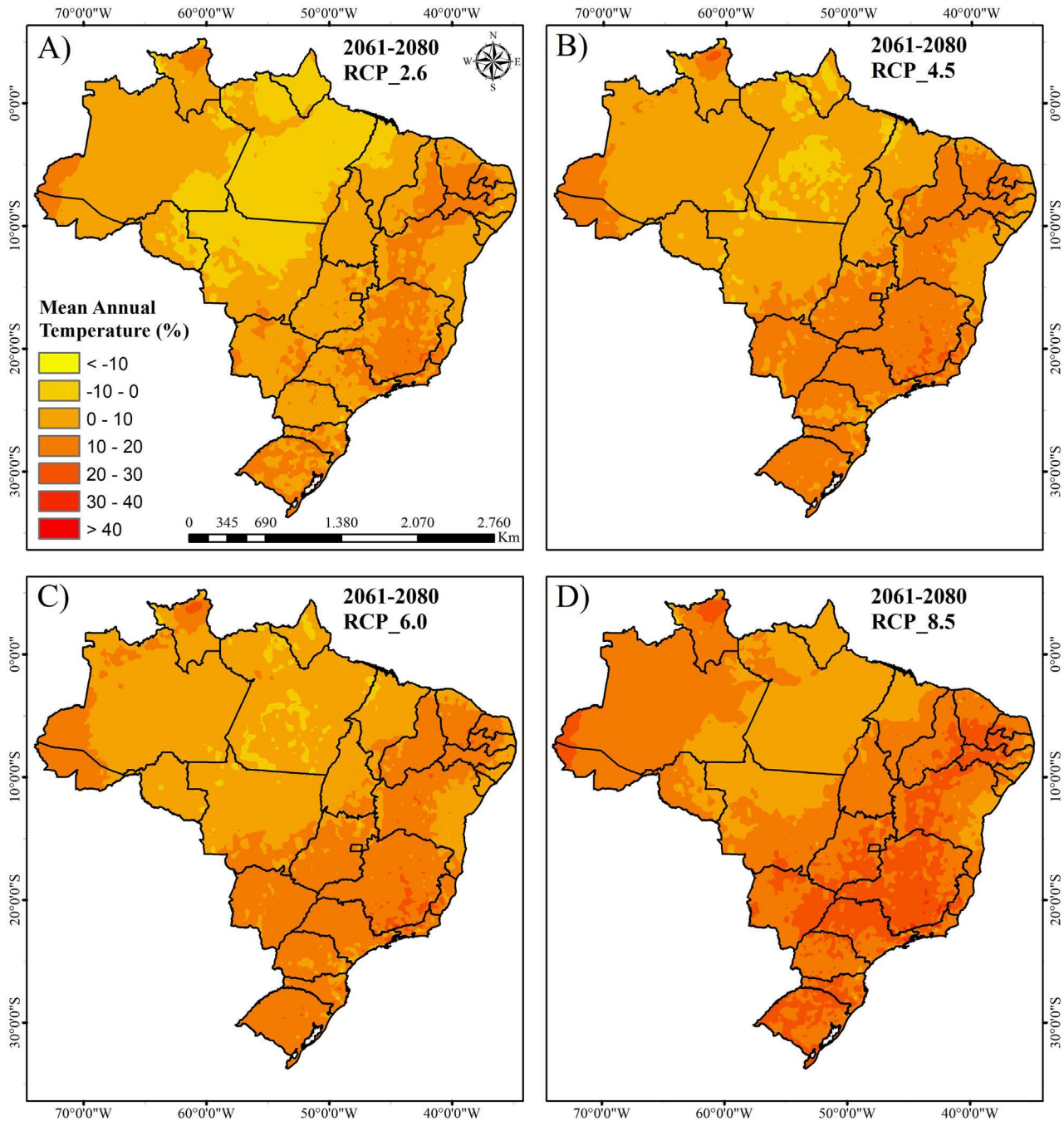
Figure 12 - Mean annual temperature variation for climate change scenarios in the period 2061-2080

respectively. Minas Gerais represents the second Brazilian state with the highest climate vulnerability related to the increase in the mean temperature (Fig. 14MG), with increases of +3.67 (23.74 ± 1.87) °C, +4.19 (24.26 ± 1.80) °C, 3.87 (23.94 ± 1.82) °C, and +4.38 (24.45 ± 1.73) °C for RCPs 2.6, 4.5, 6.0, and 8.5, respectively.

Little rainfall variation was observed for the period 2061-2080 in the Brazilian states relative to the previous period. The state of São Paulo (Fig. 15SP) presented an increase in rainfall of +83 (1471 ± 68) mm, 77 (1465 ±

72) mm, 60 (1448 ± 77) mm, and 82 (1470 ± 76) mm for RCPs 2.6, 4.5, 6.0, and 8.5 respectively, which are above those recorded for the previous period (Fig. 15SP). Paraná and the Federal District presented the highest increase in rainfall, with a slight increase for the period 2041-2060. Roraima, Rondônia, and Amapá presented the highest reductions in rainfall, with levels below those registered in the previous period. The state of Acre (Fig. 15AC) showed reductions of -443 (1842 ± 93) mm, -416 (1869 ± 88) mm, -377 (1908 ± 93) mm, and -396 (1889 ± 89) mm for
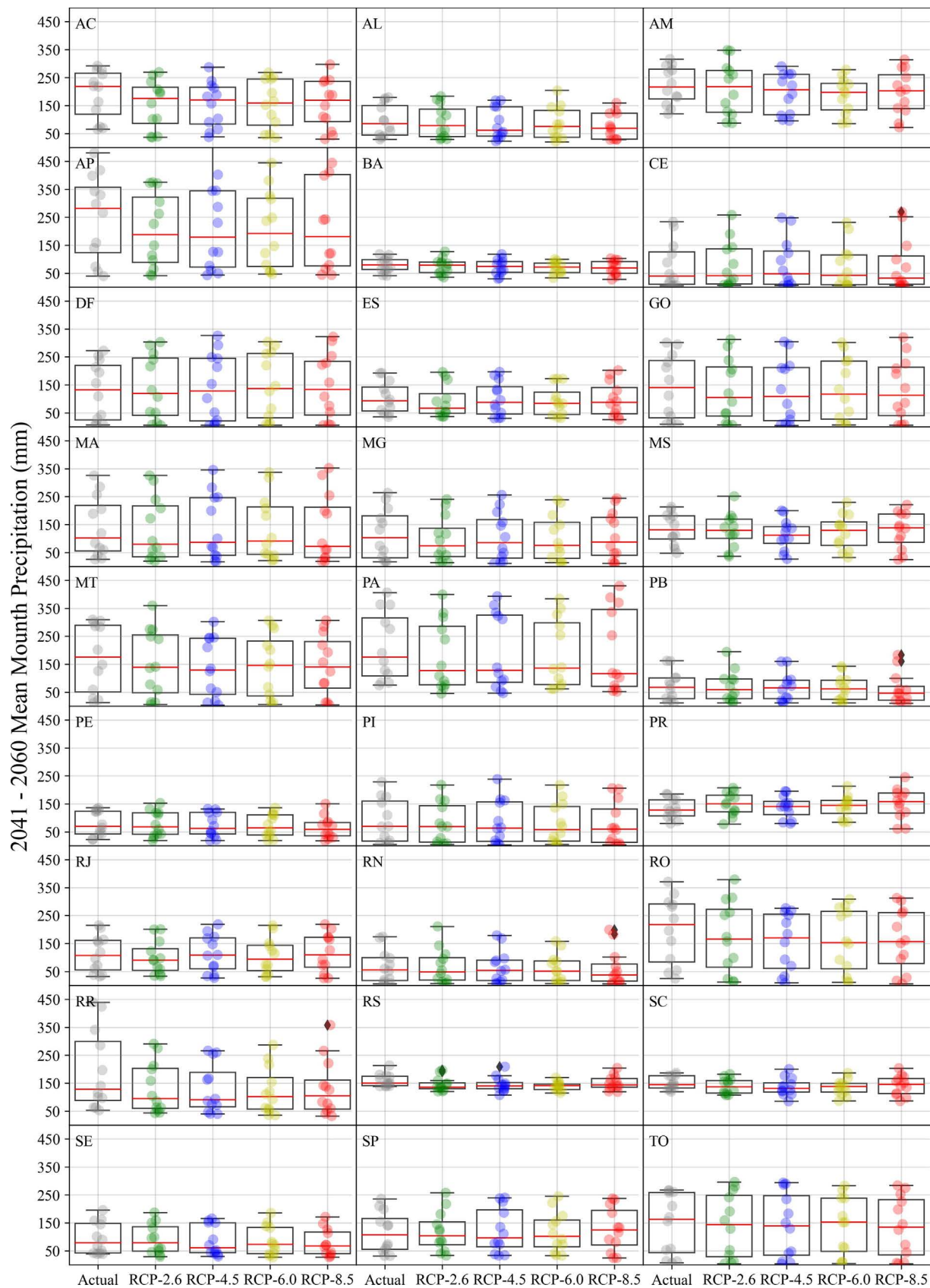
Figure 13 - Boxplot for rainfall for climate change scenarios in the period 2041-2060.
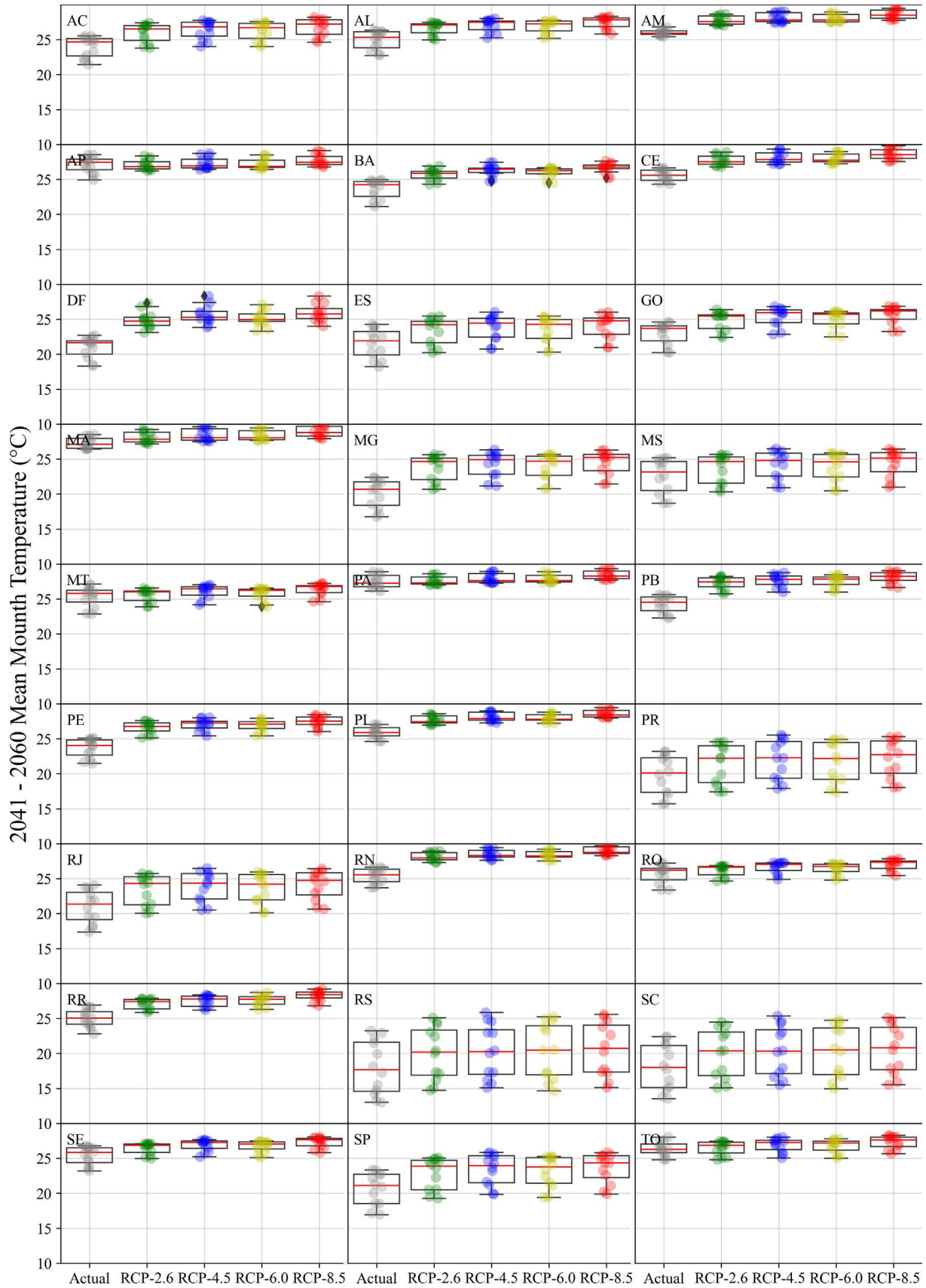
Figure 14 - Boxplot for mean air temperature for climate change scenarios in the period 2041-2060.
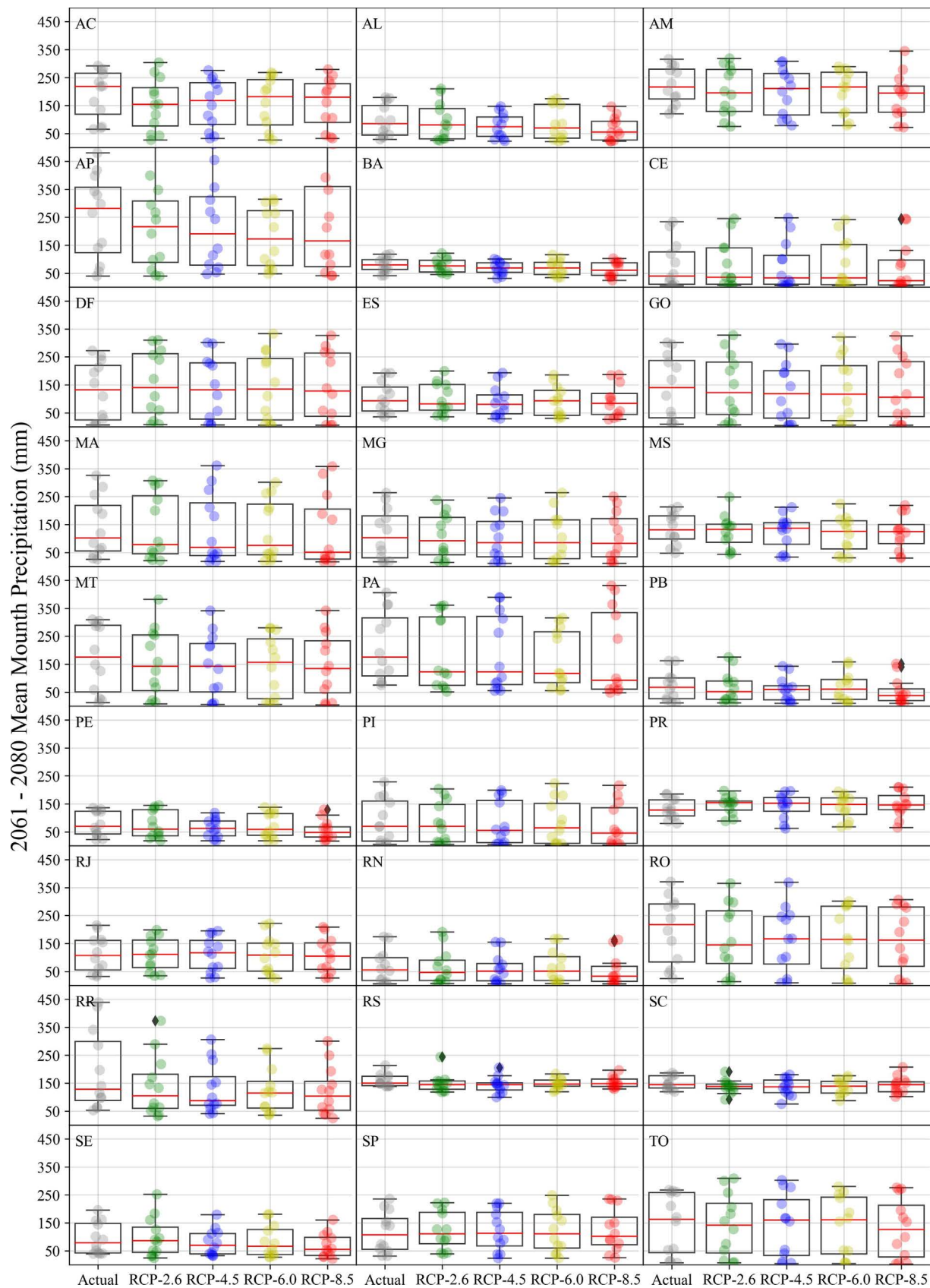
Figure 15 - Boxplot for rainfall for climate change scenarios in the period 2041-2060.
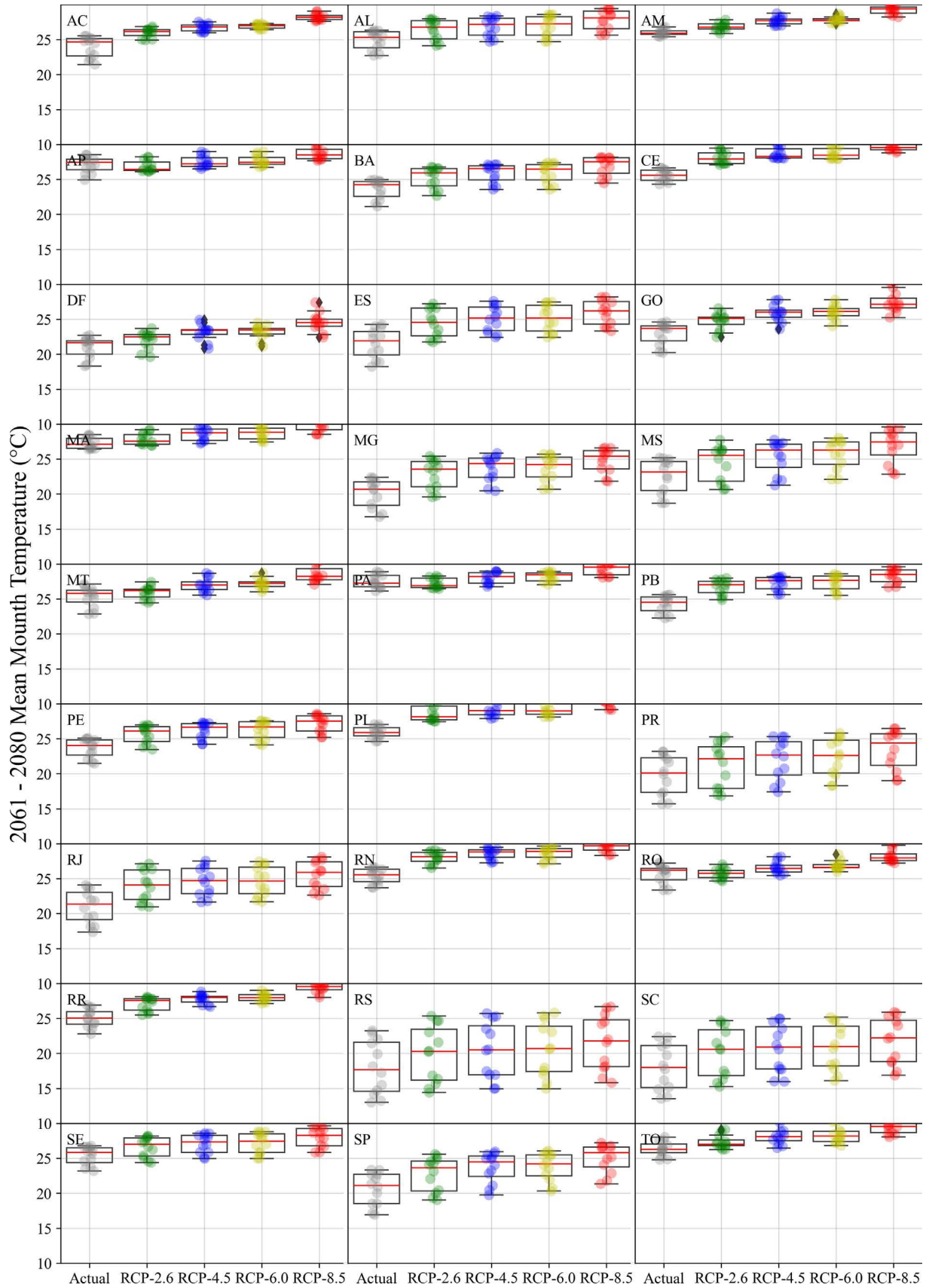
Figure 16 - Boxplot for Air Temperature in Climate Change Scenarios during the Period 2061-2080.

RCPs 2.6, 4.5, 6.0, and 8.5, respectively, which are lower than the values recorded in the previous period.

The mean temperature of the Brazilian states remained high. The state of Minas Gerais presented high means, as registered in the previous period. Piauí (Fig. 16PI) also stood out with the highest increases in the mean temperature, reaching values of +2.81 (28.72 ± 1.30) °C, +3.53 (29.44 ± 1.31) °C, 3.57 (29.49 ± 1.29) °C, and 4.91 (30.83 ± 1.38) °C for RCPs 2.6, 4.5, 6.0, and 8.5, respectively, for the period 2061-2080.

The analysis of the likely impacts of climate change on the pattern of air temperature, rainfall, evapotranspiration, soil water storage, water surplus, and monthly water deficit for the Brazilian territory in the period 2041-2060 shows an increase in the mean air temperature in both scenarios for all months (Fig. 13), with RCP 8.5 hottest among all scenarios, reaching 27.33 °C in November (Fig. 17A).

Monthly rainfall (Fig. 17B) remained below that for the current scenario for all RCPs in the assessed months. RCP 2.6 reached the highest level of monthly rainfall in January, with a value of 259 mm. Monthly evapotranspiration of RCPs was higher than the current scenario, with a variation from 88 to 134 mm for RCP 6.0 and 8.5 in June and December, respectively. The biggest surplus was registered in the 2.6 scenario, with 140 mm in January. The current scenario showed a high water surplus compared to RCPs. The monthly water deficit (Fig. 17F) was higher from March to September for all RCPs, with a value of 55 mm recorded in RCP 8.5 in August.

The period 2061-2080 (Fig. 18) showed few differences from the previous period for the monthly patterns of temperature, rainfall, evapotranspiration, soil water storage, water surplus, and water deficit in the Brazilian territory. However, RCP 8.5 stood out with a monthly increase in the mean air temperature (Fig. 18A), an increase in evapotranspiration levels (Fig. 18C), and a higher water deficit (Fig. 18D). RCP 2.6 showed an increase in the levels of water surplus (Fig. 18E) and soil water storage (Fig. 18D) compared to the other RCPs, as found in the previous period. RCP 2.6 was the most favorable scenario for the occurrence of rainfall (Fig. 18B).

Three climate zones and eight climate classes were identified under the current climate pattern condition for the Köppen-Geiger (1936) system applied in the Brazilian territory (Fig. 19). It represents one less than that recorded by Peel, Finlayson & Mcmahonet (2007), but similar to global studies carried out by Beck *et al.* (2018). Zone "A" was the most frequent, representing 82.94% of the Brazilian territory (Fig. 19), but it was not present in the states of the South region, that is, Paraná, Santa Catarina, and Rio Grande do Sul. Alvares *et al.* (2013b) found a similar result. The equatorial climate classes Af, Am, and Aw represent the most predominant classes in Brazil within zone "A" with 21.72, 28.41, and 32.80%, respectively. It

represents 82.94% (Table 1) of the territory, with higher occurrence in the North, Midwest, and Coastal regions (Fig. 15). Aparecido *et al.* (2020) showed the predominance of the climate class Aw in 58.50% of the Midwest region of Brazil.

The arid class BSh represents 3.89% (Fig. 19) of the territory, with a higher occurrence in the Northeast region. The temperate classes Cfa, Cfb, Cwa, and Cwb present 6.42, 2.38, 2.34, and 2.00% of predominance, respectively, representing a total of 13.16% (Fig. 19) of the Brazilian territory, with higher occurrence in the South and Southeast regions (Fig. 19). Dubreil *et al.* (2018) showed a variation of the temperate class for the same regions, with values of 18.8 and 16.3% for the period 1964-1989 and 1990-2015, respectively. Some studies using the Köppen-Geiger classification with the CMIP6 model can be found in the literature, but only abroad, such as the work by Hamed *et al.* (2023) for Southeast Asia.

Significant changes were found in areas of different climate classes in the four assessed scenarios, with the highest changes projected for RCP 8.5 and the lowest changes for RCP 2.6 in the period 2041-2060. The North region stands out with a higher trend to climate change for the Am class (Fig. 20). Tropical climate type "A" showed an increase in the covered area in the projected scenarios, with 87.42% for RCP 2.6 (Fig. 21A) and 88.00% for RCP 4.5 (Fig. 21B), a scenario with the highest increase in this type of climate (Fig. 22). Moreover, a predominance of 86.57% and 87.16% (Fig. 22) was observed for RCPs 6.0 (Fig. 21C) and 8.5 (Fig. 21D), respectively, with higher coverage in the North, Midwest, and Southeast regions and the coastline. This increase is caused by a reduction of areas with a predominance of temperate climate type "C".

The temperate climate type "C" presented 7.31% of predominance (Fig. 22) in RCP 2.6, the largest area among the assessed scenarios. RCPs 4.5 and 6.0 showed 6.60% and 7.18% (Fig. 22), respectively. The lowest record occurred in RCP 8.5, with 6.50% (Fig. 22), covering mainly the South and Southeast regions. The increase in the local mean temperature represents the main factor for a reduction of this climate type in the assessed RCPs.

On the other hand, the arid climate type "B" presented a significant increase in coverage in the Brazilian territory, with 5.26% in RCP 2.6 (Fig. 22). The RCP 8.5 scenario showed the highest increase in the arid climate type, with 6.33% (Fig. 22) and higher occurrence in the Northeast region, standing out for its low annual precipitation rate.

Class Af shows a reduction of geographic limits from 21.25% in RCP 2.6 to 12.54% in RCP 8.5 (Fig. 22). The Aw class presents absolute predominance in all RCPs, showing an increase in covered area from 48.92% in RCP 2.6 to 52.00% in RCP 8.5 (Fig. 22). The BSh class also had an increase in occurrence from 5.25% in RCP 2.6 to 6.09% in RCP 8.5.
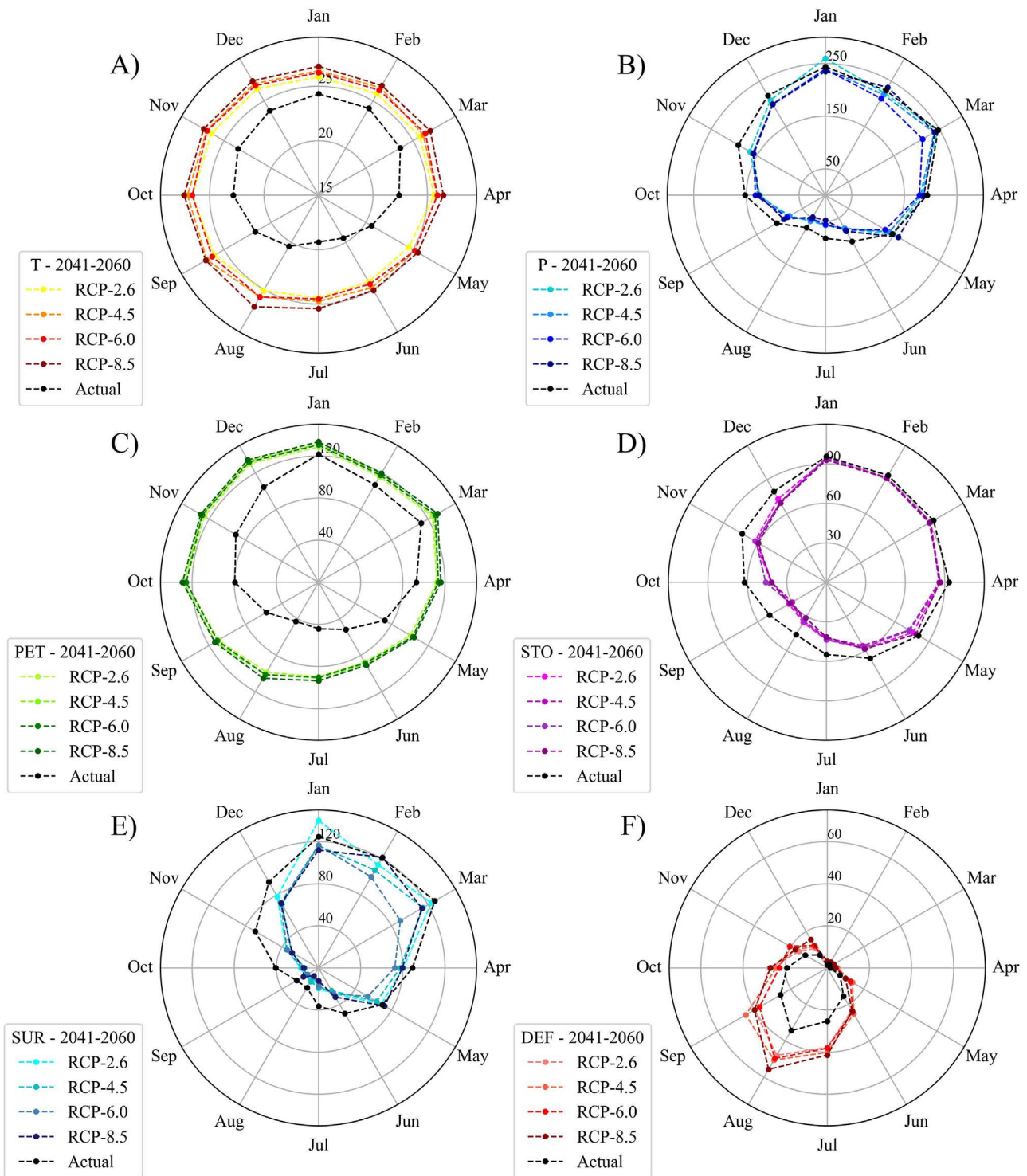
Figure 17 - Monthly variation of (A) temperature (°C) (T), (B) rainfall (mm) (P), (C) potential evapotranspiration (mm) (PET), (D) soil water storage (mm) (STO), (E) water surplus (mm) (EXC), and (F) water deficit (mm) (DEF) for the Brazilian territory in the period 2041-2060.

The BWh class only occurred in RCPs scenarios, with 0.02% in RCP 2.6 and 0.24% in RCP 8.5 and higher concentration in the extreme north of the state of Bahia. RCP 4.5 showed extinction of the climate class Cwb and a decrease in the other warm temperate classes, that is, Cfa

(6.11%) and Cfb (0.10%). RCP 8.5 also showed extinction of climate classes type "C" (Cwb and Cfb).

The Aw class stood out for the projected period from 2061 to 2080, with higher commutation in all assessed scenarios, mainly in the states of Mato Grosso, Rondônia,
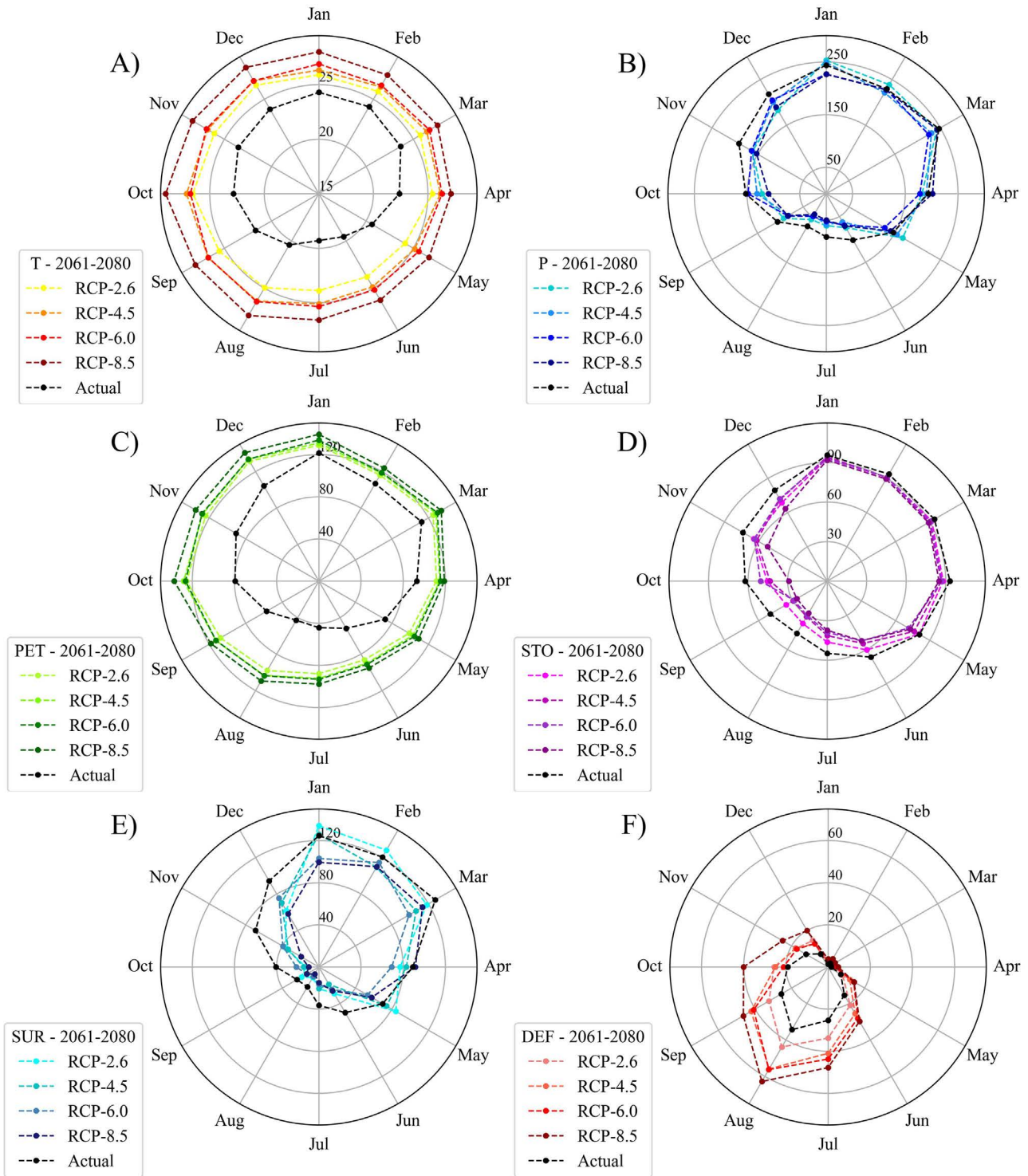
Figure 18 - Monthly variation of (A) temperature (°C) (T), (B) rainfall (mm) (P), (C) potential evapotranspiration (mm) (PET), (D) soil water storage (mm) (STO), (E) water surplus (mm) (EXC), and (F) water deficit (mm) (DEF) for the Brazilian territory in the period 2061-2080.

Mato Grosso do Sul, Minas Gerais, and São Paulo (Fig. 23). Eight climate classes were observed, with the Cwb climate class ceasing to exist in the assessed scenarios. Climate type "A" presents an expansion of the cov-

ered area for RCP 6.0 (Fig. 24C), with an increase of 1.56% (88.13%).

Climate type "C" presents an increase in the covered area in RCPs 2.6 and 4.5, with 0.81% (8.12%) and 0.29%
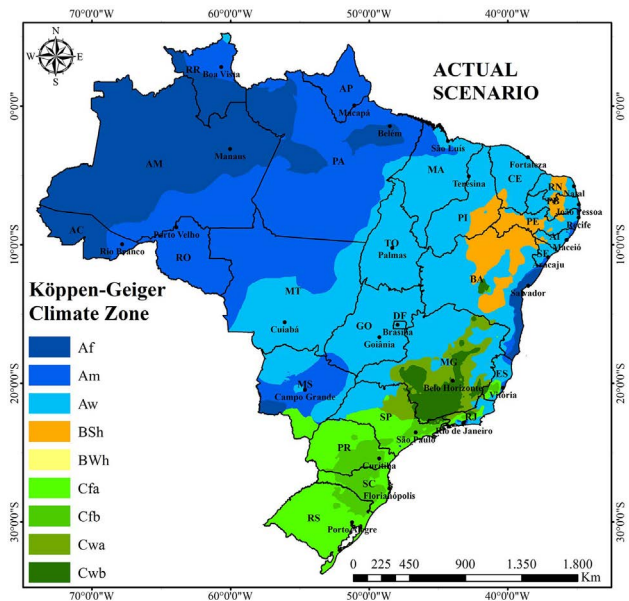
Figure 19 - Köppen-Geiger (1936) climate classification for Brazil under the current scenario.

(6.89%), respectively, and area loss for RCPs 6.0 and 8.5, with values of 0.87 (6.31%) and 0.95 (5.50%), respectively (Fig. 22), compared to the previous period. Arid climate classes "B" showed an increase in the RCP 4.5 and 8.5 scenarios, with 1.34% (6.77%) and 2.50% (8.83%), respectively, and a decrease of 0.20% (5.06%) for RCP 2.6 and 0.68% (5.54%) for RCP 6.0 (Fig. 22). Rubel and Kottek (2010) and Beck *et al.* (2018) also recorded an increase

in arid zones in global studies of climate change at the end of the century.

The BWh climate class shows a higher expansion, with values ranging from 0.08% in RCP 2.6 to 0.68% in RCP 8.5. On the other hand, classes Af and Am present a reduction in surface, with values ranging from 14.69 and 26.40% in RCP 2.6 to 12.57 and 20.43% in RCP 8.5, respectively (Fig. 22).

The Northeast region of Brazil had the occurrence of five climate classes (Af, Am, Aw, BSh, and BWh) in the assessed RCPs for the periods 2041-2060 and 2061-2080 (Figs. 21 and 24). The reduction in local rainfall and increase in temperature provided an increase in the territory coverage by the BSh and BWh climate classes in the municipalities of Petrolina and Juazeiro. The Northeast forest zone presented the Af and Am classes restricted to the coastline of the state of Bahia, mainly in the municipalities of Canavieiras, Marau, and Jaguaripe. Jenkins and Warren (2015) sought to assess the occurrence of drought events and observed an increase in their intensity and duration in the North and Northeast regions of Brazil.

The states of Paraíba and Rio Grande do Norte present a predominance of 77.40 and 89.37% of the BSh class (Table 4), respectively, for RCP 8.5 in the period 2061-2080 (Fig. 24). Bahia showed the highest climate diversity in the Northeast region, with the occurrence of five climate classes, with Aw and BSh predominating in more than 80% of the territory (Table 4) in all assessed scenarios. The BWh class, observed on the border between Bahia and Pernambuco in the future scenarios, characterizes the region of the São Francisco Valley, a fruit-producing cen-

Table 4 - Percentage of Köppen-Geiger (1936) climate classes in each Brazilian state under climate change scenarios.

| Estado	Symbol	Actual	Period 2041 0 2060				Period 2061 0 2080			
			RCP_2.6	RCP_4.5	RCP_6.0	RCP_8.5	RCP_2.6	RCP_4.5	RCP_6.0	RCP_8.5
AC	Af	80,80	14,75	17,95	12,86	9,07	0,41	7,21	6,14	12,44
AC	Am	19,20	55,00	59,43	60,43	63,32	63,51	67,46	58,21	59,44
AC	Aw	0,00	30,25	22,62	26,71	27,61	36,08	25,32	35,66	28,11
AL	Am	10,39	14,55	5,46	4,95	1,92	11,71	0,31	5,10	0,00
AL	Aw	79,54	59,42	66,82	68,70	68,04	65,30	68,30	68,20	67,19
AL	BSh	10,08	26,03	27,72	26,35	30,04	23,00	31,39	26,71	32,67
AL	BWh	0,00	0,00	0,00	0,00	0,00	0,00	0,00	0,00	0,14
AM	Af	79,33	73,03	70,39	62,99	49,90	56,30	59,37	55,77	52,99
AM	Am	20,67	26,97	29,45	36,68	49,52	43,69	40,59	43,69	44,73
AM	Aw	0,00	0,00	0,16	0,34	0,59	0,01	0,04	0,54	2,29
AP	Af	0,00	50,29	22,49	17,33	22,33	15,49	28,19	40,51	2,37
AP	Am	100,00	48,97	77,51	82,67	77,67	84,51	71,81	56,79	97,63
AP	Aw	0,00	0,73	0,00	0,00	0,00	0,00	0,00	2,70	0,00
BA	Af	8,72	10,85	6,51	5,66	3,90	8,76	6,51	6,20	2,93
BA	Am	2,15	0,53	2,62	2,86	3,15	3,19	1,62	2,22	2,17

(*continua*)

Table 4 - continua

Estado	Symbol	Actual	Period 2041 0 2060				Period 2061 0 2080			
			RCP_2.6	RCP_4.5	RCP_6.0	RCP_8.5	RCP_2.6	RCP_4.5	RCP_6.0	RCP_8.5
BA	Aw	55,12	48,73	48,21	45,85	45,37	48,30	42,88	46,40	39,38
BA	BSh	32,15	39,64	42,33	43,64	44,29	38,50	45,61	44,47	47,77
BA	BWh	0,00	0,26	0,33	1,99	3,30	1,24	3,39	0,71	7,74
BA	Cfa	0,04	0,00	0,00	0,00	0,00	0,00	0,00	0,00	0,00
BA	Cfb	0,16	0,00	0,00	0,00	0,00	0,00	0,00	0,00	0,00
BA	Cwa	0,49	0,00	0,00	0,00	0,00	0,00	0,00	0,00	0,00
BA	Cwb	1,18	0,00	0,00	0,00	0,00	0,00	0,00	0,00	0,00
CE	Aw	94,28	80,73	85,19	70,62	80,12	88,51	66,39	87,88	42,11
CE	BSh	5,72	19,27	14,81	29,38	19,88	11,49	33,61	12,12	57,89
DF	Aw	100,00	100,00	100,00	100,00	100,00	100,00	100,00	100,00	100,00
ES	Af	1,10	10,89	0,00	0,00	0,00	4,23	0,00	0,00	0,00
ES	Am	12,40	3,69	12,58	9,21	6,46	27,71	7,66	8,14	5,12
ES	Aw	55,10	84,49	86,87	89,56	93,29	66,24	92,10	91,62	94,88
ES	Cfa	16,35	0,80	0,00	0,72	0,00	1,58	0,00	0,00	0,00
ES	Cfb	9,50	0,00	0,00	0,00	0,00	0,00	0,00	0,00	0,00
ES	Cwa	0,37	0,13	0,55	0,51	0,25	0,25	0,24	0,24	0,00
ES	Cwb	5,18	0,00	0,00	0,00	0,00	0,00	0,00	0,00	0,00
GO	Am	3,97	0,00	0,00	0,00	0,00	0,44	0,00	0,00	0,00
GO	Aw	96,03	100,00	100,00	100,00	100,00	99,56	100,00	100,00	100,00
MA	Am	13,86	7,90	10,25	11,88	9,47	11,58	8,12	5,58	6,13
MA	Aw	86,14	92,10	89,75	88,08	89,71	88,42	91,87	94,42	90,68
MA	BSh	0,00	0,00	0,00	0,04	0,82	0,00	0,01	0,00	3,18
MG	Am	0,02	0,00	0,00	0,00	0,00	0,03	0,00	0,00	0,05
MG	Aw	48,68	88,43	93,04	89,78	93,71	83,26	88,81	92,08	94,72
MG	BSh	0,00	2,43	1,64	2,50	1,66	1,04	4,55	2,89	3,25
MG	Cfa	0,08	1,52	0,37	0,71	0,00	1,72	0,49	0,06	0,20
MG	Cfb	0,26	0,22	0,00	0,00	0,00	0,22	0,00	0,00	0,00
MG	Cwa	25,35	7,35	4,95	6,88	4,63	13,73	6,15	4,96	1,78
MG	Cwb	25,61	0,04	0,00	0,13	0,00	0,00	0,00	0,00	0,00
MS	Af	5,44	4,21	0,62	1,12	0,00	3,97	0,00	0,42	0,13
MS	Am	44,87	15,14	3,65	8,93	5,17	18,72	12,69	4,35	7,02
MS	Aw	39,47	80,43	95,73	89,69	94,83	76,08	87,31	95,23	92,85
MS	Cfa	10,22	0,22	0,00	0,26	0,00	1,23	0,00	0,00	0,00
MT	Am	47,55	11,06	2,46	2,73	2,61	11,88	5,71	2,52	1,06
MT	Aw	52,45	88,94	97,54	97,27	97,39	88,12	94,29	97,48	98,94
PA	Af	22,15	20,07	9,05	8,40	9,22	11,51	13,27	13,26	5,80
PA	Am	73,18	41,65	48,71	48,48	51,15	66,90	51,66	37,74	41,67
PA	Aw	4,67	38,28	42,24	43,12	39,63	21,60	35,07	48,99	52,52
PB	Am	1,11	0,35	0,00	0,05	0,00	0,12	0,00	0,02	0,00
PB	Aw	68,36	64,43	62,32	54,71	55,82	62,92	50,06	60,26	19,25
PB	BSh	30,53	35,22	37,68	45,23	44,18	36,95	49,94	39,72	77,40
PB	BWh	0,00	0,00	0,00	0,00	0,00	0,00	0,00	0,00	3,35

Table 4 - continua

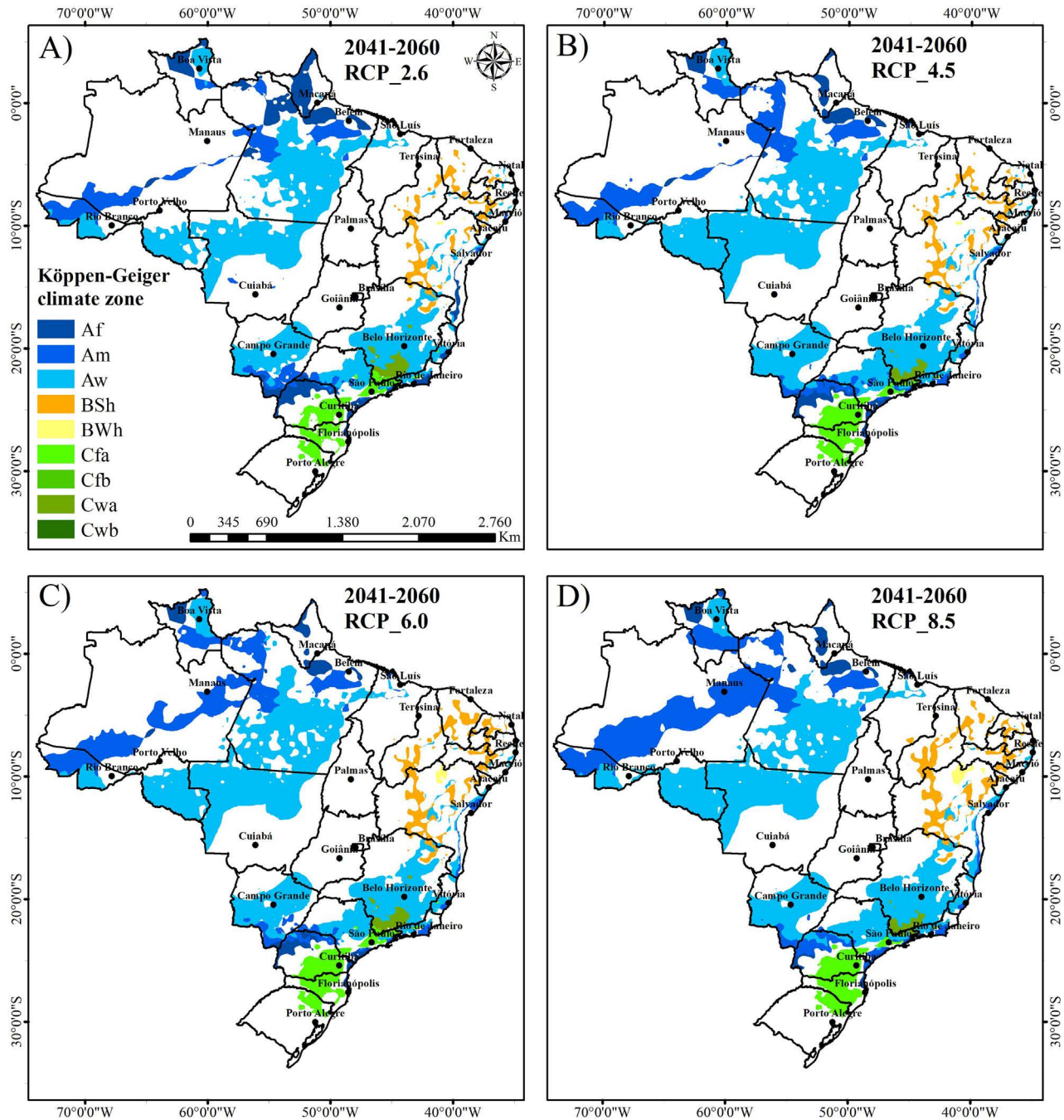| Estado	Symbol	Actual	Period 2041 0 2060				Period 2061 0 2080			
			RCP_2.6	RCP_4.5	RCP_6.0	RCP_8.5	RCP_2.6	RCP_4.5	RCP_6.0	RCP_8.5
PE	Am	4,24	4,19	2,33	2,52	1,03	3,82	0,23	2,47	0,00
PE	Aw	44,26	35,89	35,11	31,49	31,27	38,98	28,79	35,96	19,93
PE	BSh	51,50	59,92	62,51	65,31	66,14	57,13	67,88	61,56	69,10
PE	BWh	0,00	0,00	0,04	0,69	1,55	0,07	3,10	0,00	10,98
PI	Aw	80,02	72,22	73,04	68,30	62,45	70,83	69,74	75,32	46,58
PI	BSh	19,98	27,78	26,96	31,70	37,54	29,17	30,26	24,68	52,98
PI	BWh	0,00	0,00	0,00	0,00	0,01	0,00	0,00	0,00	0,44
PR	Af	0,00	25,80	20,83	17,98	5,08	20,09	4,95	15,86	21,81
PR	Am	0,11	4,14	14,86	11,15	24,24	5,83	17,80	20,18	27,28
PR	Aw	0,65	0,49	3,30	1,63	9,66	0,07	10,91	8,92	6,17
PR	Cfa	63,01	63,35	61,01	69,24	61,01	74,01	66,34	55,04	44,73
PR	Cfb	36,23	6,22	0,00	0,00	0,00	0,00	0,00	0,00	0,00
RJ	Af	0,00	18,47	0,00	0,11	0,00	7,74	0,00	0,00	0,00
RJ	Am	3,79	7,13	27,00	24,93	26,13	23,94	26,02	23,81	26,67
RJ	Aw	41,42	63,05	63,86	63,27	65,48	54,79	65,48	68,01	69,11
RJ	Cfa	25,86	10,19	5,64	8,84	3,10	12,44	6,62	5,75	2,49
RJ	Cfb	6,78	0,00	0,00	0,00	0,00	0,00	0,00	0,00	0,00
RJ	Cwa	15,08	1,17	3,50	2,86	5,29	1,08	1,88	2,44	1,73
RJ	Cwb	7,08	0,00	0,00	0,00	0,00	0,00	0,00	0,00	0,00
RN	Aw	66,21	60,71	56,33	38,01	46,12	55,47	34,97	51,59	10,63
RN	BSh	33,79	39,29	43,67	61,99	53,88	44,53	65,03	48,41	89,37
RO	Am	100,00	48,64	21,69	26,30	17,06	43,70	27,17	22,67	17,82
RO	Aw	0,00	51,36	78,31	73,70	82,94	56,30	72,83	77,33	82,18
RR	Af	58,62	71,37	51,98	46,80	37,63	35,69	59,77	48,11	28,14
RR	Am	39,49	12,49	27,43	28,75	38,79	41,95	22,57	28,04	35,01
RR	Aw	1,88	16,14	20,59	24,44	23,59	22,36	17,66	23,85	36,85
RS	Cfa	87,14	97,17	99,07	97,81	100,00	98,04	98,50	98,69	100,00
RS	Cfb	12,86	2,83	0,93	2,19	0,00	1,96	1,50	1,31	0,00
SC	Af	0,00	3,31	3,38	3,45	4,38	2,53	3,13	4,49	10,52
SC	Am	0,00	0,00	1,21	0,00	0,23	0,00	1,79	1,02	0,00
SC	Cfa	38,95	76,73	88,77	85,68	95,38	86,77	86,98	86,94	88,11
SC	Cfb	61,05	19,95	6,64	10,87	0,00	10,70	8,09	7,54	1,37
SE	Am	12,94	0,73	2,81	0,04	0,00	0,08	1,22	0,00	0,00
SE	Aw	75,78	83,75	76,42	82,20	77,31	88,47	72,72	82,28	65,72
SE	BSh	11,29	15,52	20,76	17,76	22,69	11,45	26,06	17,72	34,28
SP	Af	0,09	6,69	4,41	3,91	1,87	5,03	1,59	3,18	4,80
SP	Am	0,00	7,42	10,77	7,59	6,29	12,83	6,34	5,86	10,32
SP	Aw	31,11	60,95	66,69	64,22	75,48	50,70	71,12	76,97	78,79
SP	Cfa	37,28	24,42	16,88	23,64	13,11	30,30	19,85	11,62	4,83
SP	Cfb	11,45	0,35	0,00	0,00	0,00	0,18	0,00	0,00	0,00
SP	Cwa	16,62	0,17	1,25	0,59	3,26	0,96	1,11	2,37	1,26
SP	Cwb	3,45	0,00	0,00	0,04	0,00	0,00	0,00	0,00	0,00
TO	Am	0,00	0,00	0,00	0,00	0,00	0,00	0,00	0,00	0,00
TO	Aw	100,00	100,00	100,00	100,00	100,00	100,00	100,00	100,00	100,00

Figure 20 - Regions of climate vulnerability in the period 2041-2060.

ter of foremost importance in Brazil, with a hot desert climate with a mean annual temperature above 18 °C, a factor that can affect fruit production due to severe water restriction.

The equatorial climate type "A" predominated throughout the North region, with three climate classes (Af, Am, and Aw) in all assessed RCPs. There is a transition from the Af and Am climate zones to Aw in the south-center of the state of Acre and Pará, east of Roraima, and Rondônia, representing 28.11, 52.52, 36.85, and 82.18%

of occurrence, respectively, in RCP 8.5 in the period 2061-2080 (Table 4). There is also a predominance of Am climate zones in southern Amazonas, with 55.6% of occurrence (Table 4) for RCP 8.5 in the period 2061-2080 compared to the current scenario.

The Brazilian Midwest showed a predominance of climate classes Af, Am, Aw, and Cfa in most RCPs, with the Cfa class present in RCPs 2.6 and 6.0 for the periods 2041-2060 (Figs. 21A and C) and 2061-2080 (Fig. 24A), located in the extreme south of the state of Mato Grosso
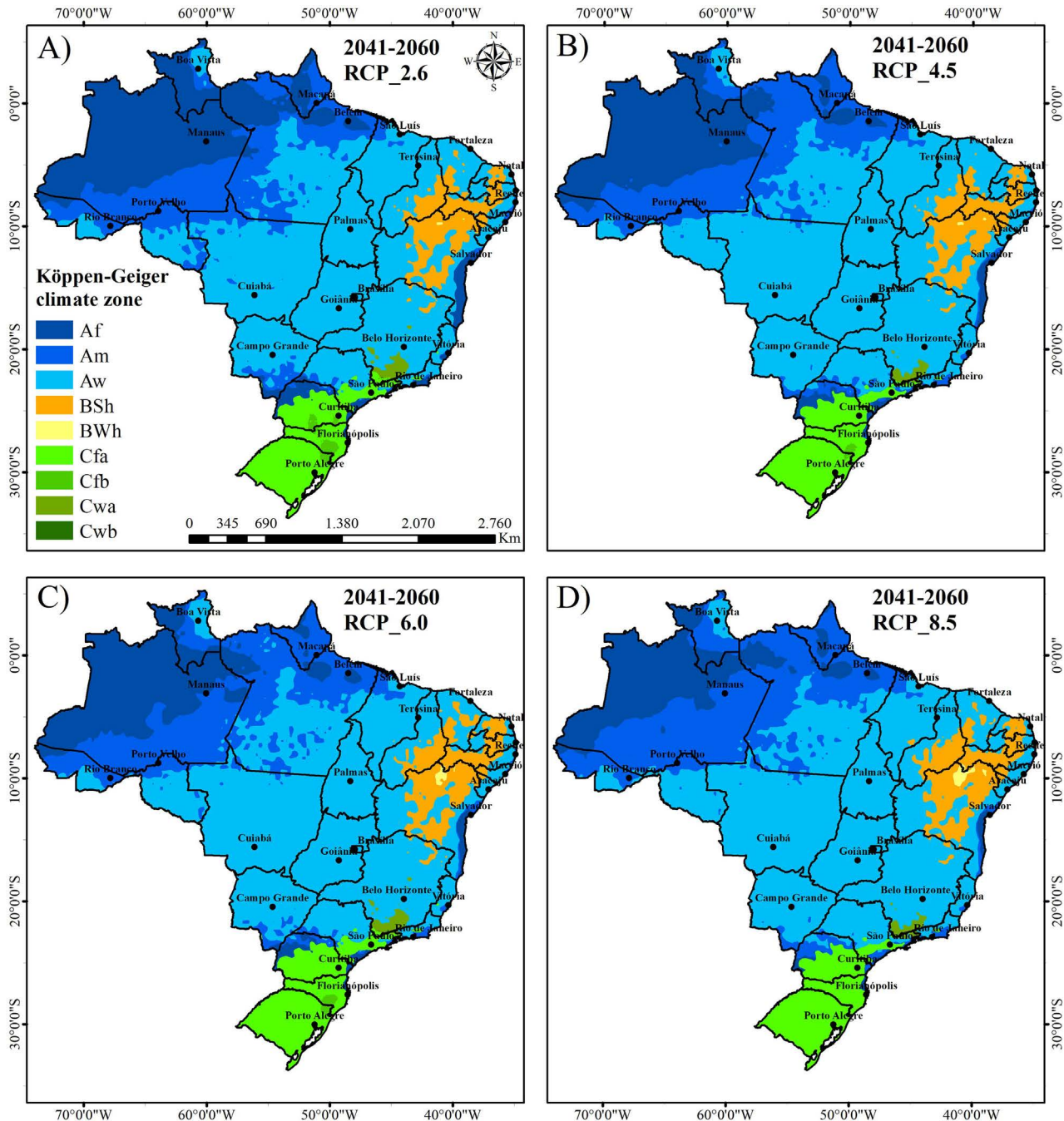
Figure 21 - Köppen-Geiger (1936) climate classification for Brazil in the period 2041-2060.

do Sul, with a predominance of 0.22 to 1.23% (Table 4) mainly in the municipalities of Paranhos and Ponta-Porã. The Aw climate class has a higher predominance in RCP 8.5 for the period 2061-2080 (Fig. 24D), with 100% in Goiás, 92.85% in Mato Grosso do Sul, and 98.94% in Mato Grosso (Table 4). This expansion is directly related to a decrease in local rainfall rates.

The Cfb class in the South of Brazil remains restricted to the southeast of Santa Catarina on the border with Rio Grande do Sul, with 1.37% (Table 4) of occurrence in

RCP 8.5 for the period 2061-2080 relative to the current scenario (Fig. 24D). The rest of the state showed a predominance of the Cfa class, as well as the entire state of Rio Grande do Sul and the center-south of Paraná. The northern Paraná concentrates the climate classes Am, Aw, and Af.

The Brazilian Southeast region presented the occurrence of eight climate classes (Am, Aw, BSh, BWh, Cfa, Cfb, Cwa, and Cwb) in the assessed RCPs. There is a reduction in areas with warm temperate cli-
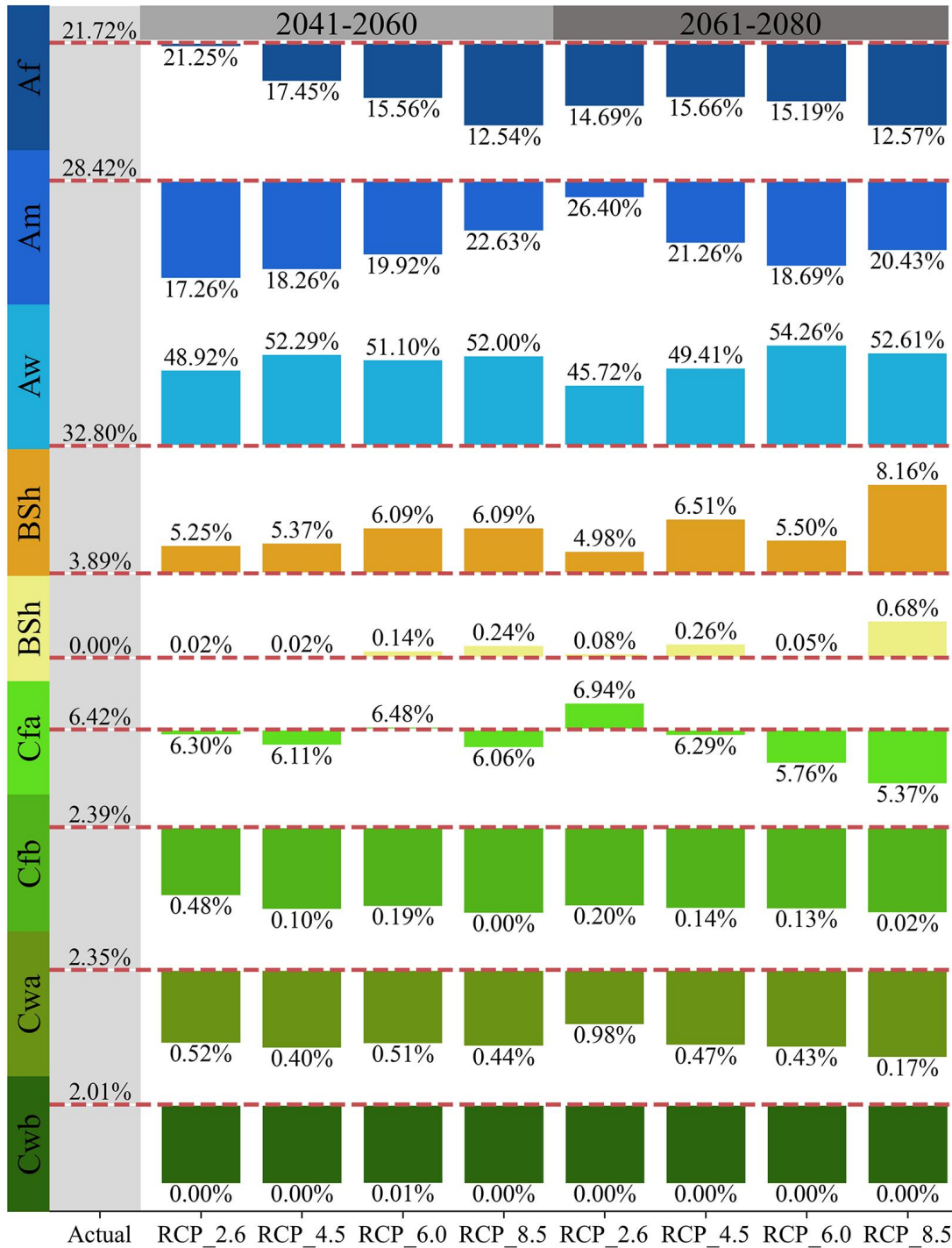
Figure 22 - Prevalence of Köppen climate classes within each scenario.

mate classes (Cfa, Cfb, Cwa, and Cwb) and the Am class, with higher occurrence in the south of the State of São Paulo in RCP 8.5 for the period 2061-2080 (Fig. 24D) compared to the current period. The state of Minas Gerais showed an increase in areas with classes Aw and BSh, representing 94.72 and 3.25% (Table 4), respectively. Tavares *et al.* (2018) assessed the negative

impacts on coffee production in the Southeast region using future scenarios for the end of the century, showing a potential loss of yield of 25%, a factor conditioned by an increase in areas with high climate risk due to an increase in the mean temperature.

The decreased rainfall in the assessed scenarios, associated with an increase in the mean air temperature,
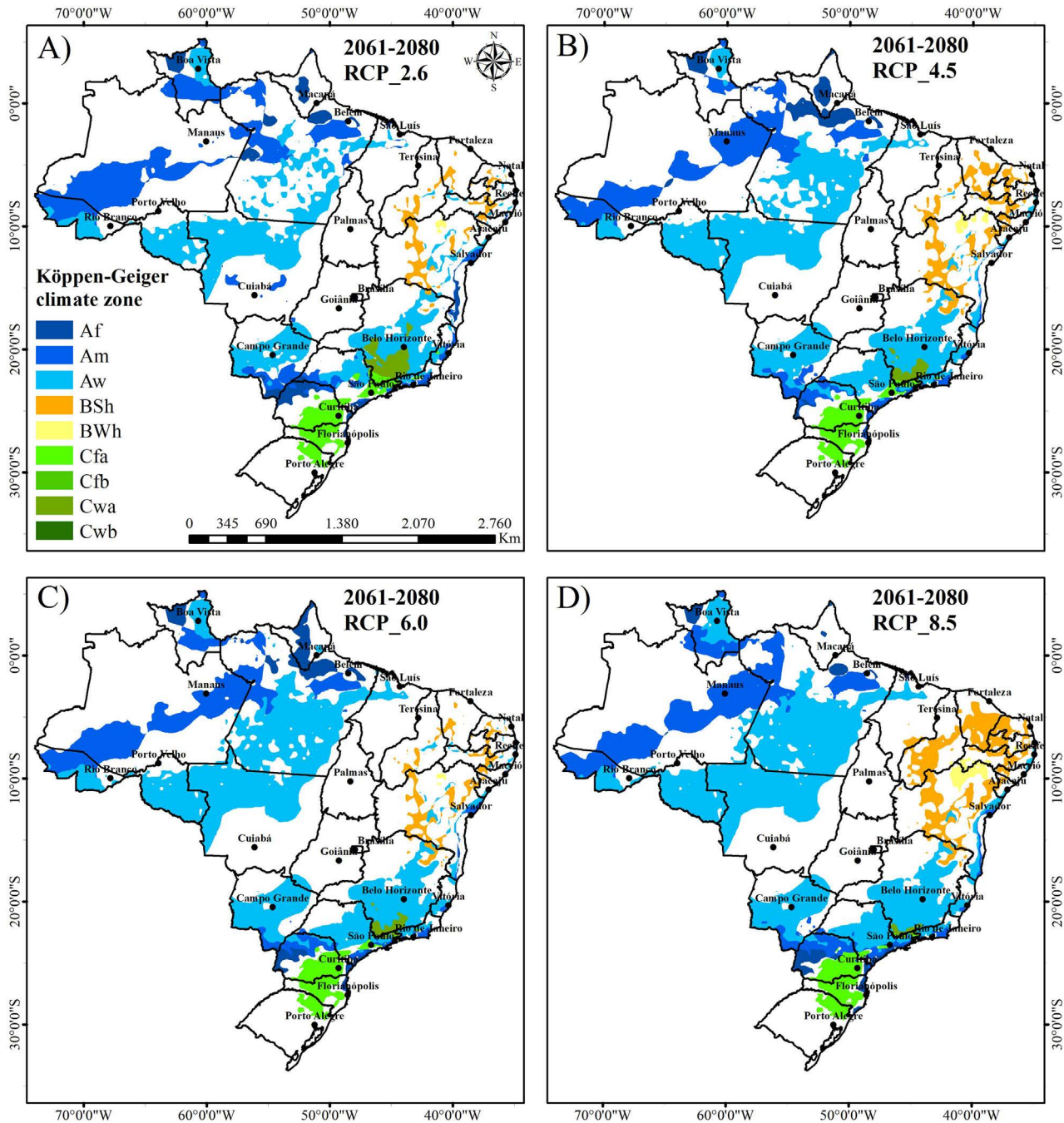
Figure 23 - Regions of climate vulnerability in the period 2061-2080.

represents factors closely related to crop development and yield. Assad *et al.* (2019) observed an increase in Brazil's vulnerability as the world's largest food supplier given the 4 °C increase in the mean temperature. Changes in climate patterns can directly affect the economic development of Brazil due to the negative effects of crops. According to Santos *et al.* (2021), higher economic losses are projected for locations with an economy dependent on agriculture, especially soybean, such as the central regions of the Mid-west and part of the Northeast. Souza and Haddad (2021)

predicted future losses of Brazilian gross domestic pro-duct, ranging from 0.4 to 1.8% at the end of the century due to climate change.

4. Conclusions

The conclusion highlights the significant impacts of climate change on the Brazilian territory, as projected by the BCC-CSM1-1 model under different Representative Concentration Pathway (RCP) scenarios. The study inves-
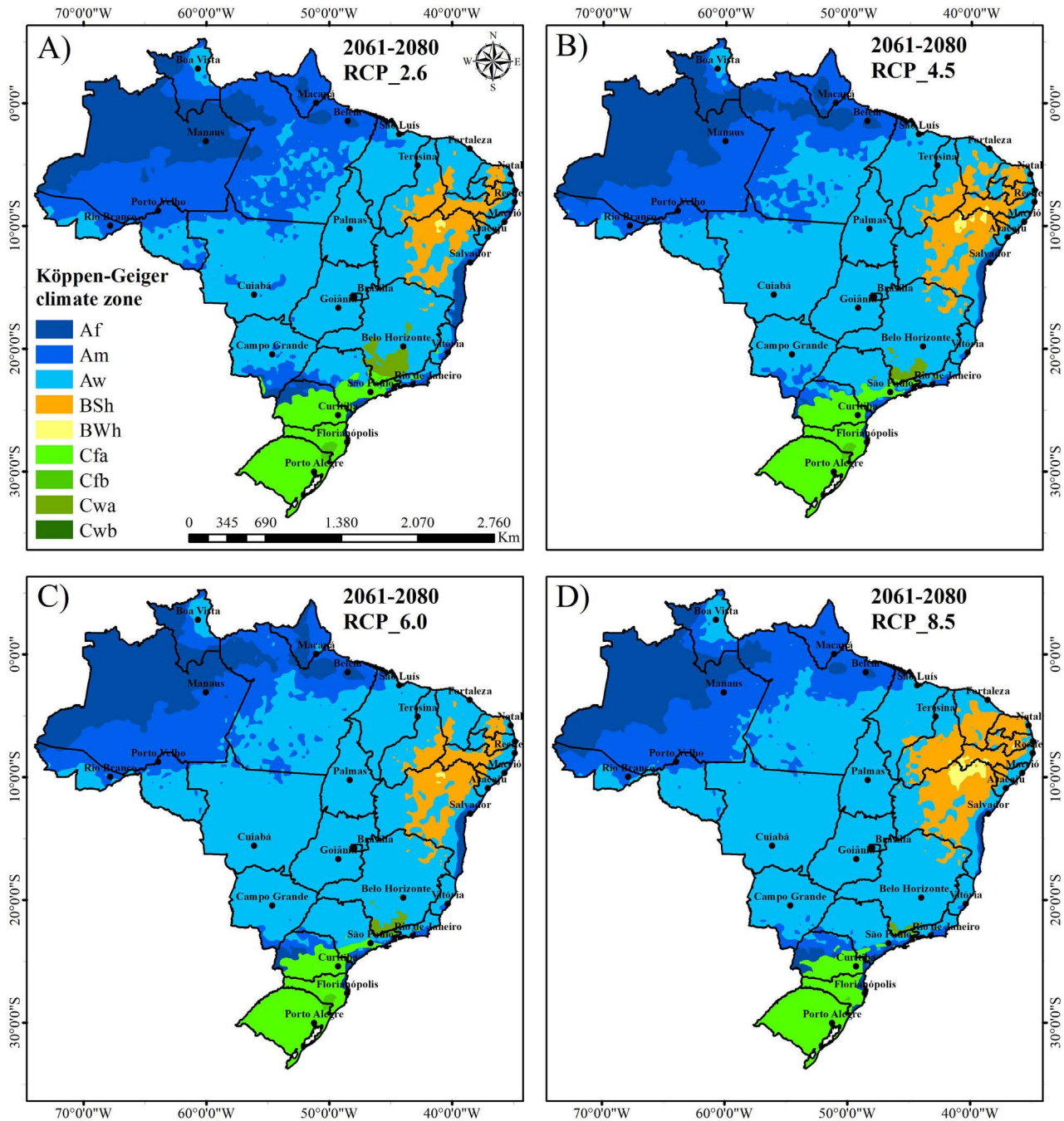
Figure 24 - Köppen-Geiger (1936) climate classification for Brazil in the period 2061-2080.

tigated eight Köppen-Geiger climate classes in the region for the current scenario (1989-2019), with Af, Am, and Aw classes being the most predominant, particularly in the North, Midwest, and Southeast regions.

The climate change scenarios analyzed indicate potential shifts in the distribution of climate classes, with an increase in arid climate zones BSh and BWh in the Northeast region of Brazil. This change may lead to an increased demand for irrigation in affected areas. Additionally, there is a reduction in the Af class and temperate classes "C" in the future scenarios. The Aw class remains predominant in all assessed scenarios.

The findings suggest that in the coming decades, climate change is likely to bring significant alterations in temperature and/or rainfall patterns, potentially impacting the overall climate conditions in the country. These changes could have substantial implications for agriculture, water resources, and ecosystems, necessitating adaptive measures and informed decision-making to address the challenges posed by these shifts.

Overall, the study underscores the importance of understanding and preparing for the potential impacts of climate change on Brazil's climate and ecosystems, providing valuable insights for policymakers, researchers, and stakeholders to develop effective strategies for climate resilience and sustainable development.

Acknowledgment

References

ADEFISAN, E. Climate change inpact on rainfall and temperature distributions over west africa from three IPCC scenarios. **Journal of Earth Science & Climate Change**, v. 9, n. 6, p. 476, 2018. doi

ALMEIDA, A.Q.; SOUZA, R.M.S.; LOUREIRO, D.C.; PEREIRA, D.R.; CRUZ, M.A.S.; *et al.* Modeling the spatial dependence of the rainfall erosivity index in the Brazilian semiarid. **Pesquisa Agropecuária Brasileira**, v. 52, n. 6, p. 371-379, 2017. doi

ALVARES, C.A.; STAPE, J.L.; SENTELHAS, P.C.; DE MORAES GONÇALVES, J.L. Modeling monthly mean air temperature for Brazil. **Theoretical and Applied Climatology**, v. 113, n. 1, p. 407-427, 2013a. doi

ALVARES, C.A.; STAPE, J.L.; SENTELHAS, P.C.; GONÇALVES, J.L.M.; SPAROVEK, G. Köppen's climate classification map for Brazil. **Meteorologische Zeitschrift**, v. 22, n. 6, p. 711-728, 2013b.

APARECIDO, L.E.O.; MORAES, J.R.S.C.; MENESES, K.C.; TORSONI, G.B.; LIMA, R.F.; *et al.* Köppen-Geiger and Camargo climate classifications for the Midwest of Brasil. **Theoretical and Applied Climatology**, v. 142, n. 3, p. 1133-1145, 2020. doi

ARGUEZ, A.; DURRE, I.; APPLEQUIST, S.; VOSE, R.S.; SQUIRES, M.F.; *et al.* NOAA's 1981-2010 US climate normals: An overview. **Bulletin of the American Meteorological Society**, v. 93, n. 11, p. 1687-1697, 2012. doi

AYOADE, J.O. **Introdução à Climatologia para os Trópicos**. Rio de Janeiro: Bertrand Brasil, 2010.

BECK, H.E.; ZIMMERMANN, N.E.; MCVICAR, T.R.; VERGOPOLAN, N.; BERG, A.; *et al.* Present and future Köppen-Geiger climate classification maps at 1-km resolution. **Scientific Data**, v. 5, n. 1, p. 1-12, 2018. doi

BELDA, M.; HOLTANOVÁ, E.; HALENKA, T.; KALVOVÁ, J. Climate classification revisited: From Köppen to Trewartha. **Climate Research**, v. 59, n. 1, p. 1-13, 2014. doi

BELDA, M.; HOLTANOVA, E.; HALENKA, T.; KALVOVA, J. Vegetation zones in changing climate. In: **EGU General Assembly Conference Abstracts**, Göttingen, p. 18958, 2017

BRUNO, R.A.L. **Um Brasil Ambivalente: Agronegócio, Ruralismo e Relações de Poder**. Rio de Janeiro: Mauad Editora Ltda, 2019.

CAMARGO, A. São Paulo State Water Balance. **Bol. Inst. Agronômico Camp.**, v. 116, n. 1, p. 1-24, 1971.

CAMARGO, A.P. Climatic classification for zoning of agroclimatic aptitude. **Brazilian Journal of Agrometeorology**, v. 8, n. 1, p. 126-131, 1991.

CANDOLLE, A. **Geographie Botanique Raisonnee**. Geneve: V. Masson, 1874.

CASAROLI, D.; ROSA, F.D.O.; ALVES JÚNIOR, J.; EVANGELISTA, A.W.P.; BRITO, B.V.D.; *et al.* Aptidão edafoclimática para o mogno-africano no Brasil. **Ciência Florestal**, v. 28, n. 1, p. 357-368, 2018. doi

CORNELL, J.A.; BERGER, R.D. Factors that influence the value of the coefficient of determination in simple linear and nonlinear regression models. **Phytopathology**, v. 77, n. 1, p. 63-70, 1987.

COUTINHO, L. **Biomas Brasileiros**. São Paulo: Oficina de Textos, 2016.

DABANLI, I. Temperature difference relationship among precipitation, dry days, and spells in Turkey. **Theoretical and Applied Climatology**, v. 135, n. 1-2, p. 765-772, 2019. doi

DE CARVALHO, L.G.; DE CARVALHO A.M.; DE OLIVEIRA, M.S.; VIANELLO, R.L.; SEDIYAMA, G.C.; *et al.* Multivariate geostatistical application for climate characterization of Minas Gerais State, Brazil. **Theoretical and Applied Climatology**, v. 102, n. 3-4, p. 417-428, 2010. doi

DE CASTRO, M.; GALLARDO, C.; JYLHA, K.; TUOMENVIRTA, H. The use of a climate-type classification for assessing climate change effects in Europe from an ensemble of nine regional climate models. **Climatic Change**, v. 81, n. 1, p. 329-341, 2007. doi

DUBREUIL, V.; FANTE, K.P.; PLANCHON, O.; SANT'ANNA NETO, J.L. Climate change evidence in Brazil from Köppen's climate annual types frequency. **International Journal of Climatology**, v. 39, n. 3, p. 1446-1456, 2019. doi

FATHI, M.T.; EZZIYYANI, M. How can data mining help us to predict the influence of climate change on Mediterranean agriculture? **International Journal of Sustainable Agricultural Management and Informatics**, v. 5, n. 2-3, p. 168-180, 2019. doi

FERNANDEZ, J.P.; FRANCHITO, S.H.; RAO, V.B.; LLOPART, M. Changes in Koppen-Trewartha climate classification over South America from RegCM4 projections. **Atmospheric Science Letters**, v. 18, n. 11, p. 427-434, 2017. doi

FLOHN, H. Neue Anschauungen über die allgemeine zirkulation der atmosphareund ihre klimatische bedeutung. **Erdkunde**, v. 4, n. 3, p. 141-162, 1950.

GALLARDO, C.; GIL, V.; HAGEL, E.; TEJEDA, C.; DE CASTRO, M. Assessment of climate change in Europe from an ensemble of regional climate models by the use of Köppen-Trewartha classification. **International Journal of Climatology**, v. 33, n. 9, p. 2157-2166, 2013. doi

GEIGER, R. **Überarbeitete Neuausgabe von Geiger, R. Köppen-Geiger/Klima der Erde. (Wandkarte 1: 16 Mill).** Gotha: Klett-Perthes, 1961.

GONÇALVES, F.N.; BACK, A.J. Analysis of spatial and seasonal variation and precipitation trends in southern Brazil. **Revista de Ciências Agrárias**, v. 41, n. 3, p. 592-602, 2018. doi

HAMED, M.M.; NASHWAN, M.S.; SHAHID, S.; WANG, X.J.; ISMAIL, T.B. *et al.* Future Köppen-Geiger climate zones

over Southeast Asia using CMIP6 Multimodel Ensemble. **Atmospheric Research**, v. 283,106560, 2023. doi

HE, Q.; SILLIMAN, B.R. Climate change, human impacts, and coastal ecosystems in the Anthropocene. **Current Biology**, v. 29, n. 19, p. 1021-1035, 2019.

HOLDRIDGE, L.R. **Life Zone Ecology**. San Jose: Tropical Science Center, 1967.

IBGE. **Anuário Estatístico do Brasil**. Rio de Janeiro: IBGE, 2011.

INTERGOVERNMENTAL PANEL ON CLIMATE CHANGE (IPCC). **Managing the Risks of Extreme Events and Disasters to Advance Climate Change Adaptation. A Special Report of Working Groups I and II of the Intergovernmental Panel on Climate Change**. Cambridge: Cambridge University Press, 2012.

INTERGOVERNMENTAL PANEL ON CLIMATE CHANGE (IPCC). **Climate Change 2014: Synthesis Report. Contribution of Working Groups I, II and III to the Fifth Assessment Report of the Intergovernmental Panel on Climate Change**. Cambridge: Cambridge University Press, 2014

INTERGOVERNMENTAL PANEL ON CLIMATE CHANGE (IPCC). **Climate Change 2013: The Physical Science Basis. Contribution of Working Group I to the Fifth Assessment Report of the Intergovernmental Panel on Climate Change.** Cambridge: Cambridge University Press, 2013.

JENKINS, K.; WARREN, R. Quantifying the impact of climate change on drought regimes using the Standardised Precipitation Index. **Theoretical and Applied Climatology**, v. 120, n. 1, p. 41-54, 2015. doi

KARGER, D.N.; CONRAD, O.; BÖHNER, J.; KAWOHL, T.; KREFT, H.; *et al.* Climatologies at high resolution for the earth's land surface areas. **Scientific Data**, v. 4, n. 1, p. 1-20, 2017. doi

KING, M.; ALTDORFF, D.; LI, P.; GALAGEDARA, L.; HOLDEN, J.; *et al.* Northward shift of the agricultural climate zone under 21 st-century global climate change. **Scientific Reports**, v. 8, n. 1, p. 7904, 2018. doi

KÖPPEN, W. **Das Geographische System der Klimatologie**. Berlin: Gebrüdcr Borntraeger, 1936.

KRIGE, D.G. A statistical approach to some basic mine valuation problems on the Witwatersrand. **Journal of the Southern African Institute of Mining and Metallurgy**, v. 52, n. 6, p. 119-139, 1951.

KRITICOS, D.J.; WEBBER, B.L.; LERICHE, A.; OTA, N.; MACADAM, I.; *et al.* CliMond: Global high resolution historical and future scenario climate surfaces for bioclimatic modelling. **Methods in Ecology and Evolution**, v. 3, n. 1, p. 53-64, 2012. doi

LEAO, S. Mapping 100 years of Thornthwaite moisture index: impact of climate change in Victoria, Australia. **Geographical Research**, v. 52, n. 3, p. 309-327, 2014. doi

LEHNER, F.; FORMAYER, H. Insights on the climate of Bhutan from a new daily 1 km gridded data set for temperature and precipitation. **International Journal of Climatology**, v. 43, n. 11, p. 4927-4943, 2023. doi

LITKE, N.A.; POß-DOERING, R.; FEHRER, V.; KÖPPEN, M.; KÜMMEL, S.; *et al.* Building climate resilience: Awareness of climate change adaptation in German Primary Care. **Research Square**, Preprint, 2023. doi

LORI, M.; SYMNACZIK, S.; MÄDER, P.; DE DEYN, G.; GATTINGER, A. Organic farming enhances soil microbial abundance and activity - A meta-analysis and meta-regression. **PLoS One**, v. 12, n. 7, p. e0180442, 2017. doi

LUÍS, J.C. **Impactos das Mudanças Climáticas Projetadas na Distribuição de Espécies Arbóreas no Sudoeste de Angola**. Tese de Doutorado, Universidade de Lisboa, 2020.

MARTINS, F.B.; GONZAGA, G.; DOS SANTOS, D.F.; REBOITA, M.S. Classificação climática de Köppen e de Thornthwaite para Minas Gerais: cenário atual e projeções futuras. **Revista Brasileira de Climatologia**, v. 1, 60896, 2018. doi

MEDEIROS, R.M.; CAVALCANTI, E.P.; DUARTE, J.F.M. Classificação climática de Köppen para o estado do Piauí-Brasil. **Revista Equador**, v. 9, n. 3, p. 82-99, 2020. doi

MEDEIROS, S.D.S.; CECÍLIO, R.A.; JÚNIOR, J.C.M.; JUNIOR, J.L.S. Estimativa e espacialização das temperaturas do ar mínimas, médias e máximas na Região Nordeste do Brasil. **Revista Brasileira de Engenharia Agrícola e Ambiental**, v. 9, p. 247-255, 2005. doi

MIAO, C.; DUAN, Q.; SUN, Q.; HUANG, Y.; KONG, D.; *et al.* Assessment of CMIP5 climate models and projected temperature changes over Northern Eurasia. **Environmental Research Letters**, v. 9, n. 5, p. 055007, 2014. doi

MIHAILOVIC, D.T.; LALIC, B.; DRESKOVIC, N.; MIMIC, G.; DJURDJEVIC, V.; *et al.* M. Climate change effects on crop yields in Serbia and related shifts of Köppen climate zones under the SRES A1B and SRES A2. **International Journal of Climatology**, v. 35, n. 11, p. 3320-3334, 2015. doi

NASCIMENTO, D.T.F.; LUIZ, G.C.; OLIVEIRA, I.J.D. Panorama dos sistemas de classificação climática e as diferentes tipologias climáticas referentes ao Estado de Goiás e ao Distrito Federal (Brasil). **Elisee: Revista de Geografia da UEG**, v. 5, n. 2, p. 59-86, 2016.

NETZEL, P.; STEPINSKI, T. On using a clustering approach for global climate classification. **Journal of Climate**, v. 29, n. 9, p. 3387-3401, 2016. doi

O'NEILL, B.C.; TEBALDI, C.; VAN VUUREN, D.P.; EYRING, V.; FRIEDLINGSTEIN, P.; *et al.* The scenario model intercomparison project (ScenarioMIP) for CMIP6. **Geoscientific Model Development**, v. 9, n. 9, p. 3461-3482, 2016. doi

PECL, G.T.; ARAÚJO, M.B.; BELL, J.D.; BLANCHARD, J.; BONEBRAKE, T.C.; *et al.* Biodiversity redistribution under climate change: impacts on ecosystems and human well-being. **Science**, v. 355, n. 6332, eaai9214, 2017. doi

PEEL, M.C.; FINLAYSON, B.L.; MCMAHON, T.A. Updated world map of the Köppen-Geiger climate classification. **Hydrology and Earth System Sciences**, v. 11, n. 5, p. 1633-1644, 2007. doi

RAHIMI, J.; LAUX, P.; KHALILI, A. Assessment of climate change over Iran: CMIP5 results and their presentation in terms of Köppen-Geiger climate zones. **Theoretical and Applied Climatology**, v. 141, n. 1, p. 183-199, 2020. doi

REBOUÇAS, A.C. Água no Brasil: Abundância, desperdício e escassez. **Bahia Análise & Dados**, v. 13, n. 1, p. 341-345, 2003.

RIGAL, A; AZAÏS, J.M.; RIBES, A. Estimating daily climatological normals in a changing climate. **Climate Dynamics**, v. 53, n. 1, p. 275-286, 2019. doi

RODRIGUES, G.S.; PUTTI, F.F.; SILVA, A.C.; OLIVEIRA, A.S.; FILHO, L.R.A.G. Climatological hydric balance and the trends analysis climatic in the region of Machado in Minas Gerais State, Brazil. **American Journal of Climate Change**, v. 7, n. 4, p. 558-574, 2018.

ROLIM G.S.; APARECIDO L.E.O.; SOUZA P.S.; AUGUSTO R.; LAMPARELLI C.; *et al.* Climate and natural quality of Coffea arabica L. drink. **Theoretical and Applied Climatology**, v. 141, n. 1, p. 87-98, 2020. doi

ROLIM, G.S.; APARECIDO, L.E.O. Camargo, Köppen and Thornthwaite climate classification systems in defining climatical regions of the state of São Paulo, Brazil. **International Journal of Climatology**, v. 36, n. 2, p. 636-643, 2016. doi

RUBEL, F.; KOTTEK, M. Observed and projected climate shifts 1901-2100 depicted by world maps of the Köppen-Geiger climate classification. **Meteorologische Zeitschrift**, v. 19, n. 2, p. 135-141, 2010. doi

RUMAN, A. Modelling climate types in South Pannonian Basin, Serbia by applying the Köppen-Geiger climate classification. **Modeling Earth Systems and Environment**, v. 6, n. 3, p. 1303-1313, 2020. doi

SAIFUDEEN, A.; RAO, R.R.; MANI, M. Reassessing climate classification for buildings under climate change: Indian context. **World Development Sustainability**, v. 2, 100053, 2023. doi

SANDERSON, B.M.; KNUTTI, R.; CALDWELL, P. representative democracy to reduce interdependency in a multi-model ensemble. **Journal of Climate**, v. 28, n. 13, p. 5171-5194, 2015. doi

SAUER, S.; LEITE, S.P. Agrarian structure, foreign investment in land, and land prices in Brazil. **The Journal of Peasant Studies**, v. 39, n. 3-4, p. 873-898, 2012. doi

SETZER, J. **Atlas Climático e Ecológico do Estado de São Paulo**. São Paulo: Comissão Interestadual da Bacia Paraná-Uruguai, p. 61, 1966.

SILVA, J.A.N.; SALES, M.C.L. Considerações sobre a aplicabilidade da classificação climática de Thornthwaite no contexto semiárido do Nordeste Brasileiro: estudo de caso da Serra de Baturité e seu entorno. **Revista Brasileira de Climatologia**, v. 26, n. 1, p. 833-853, 2020. doi

SKALÁK, P.; FARDA, A.; ZAHRADNÍCEK, P.; TRNKA, M.; HLÁSNY, T.; *et al.* Projected shift of Köppen-Geiger zones in the central Europe:a first insight into the implications for ecosystems and the society. **International Journal of Climatology**, v. 38; n. 9, p. 3595-3606, 2018. doi

SRIVASTAVA, A.K.; MBOH, C.M.; ZHAO, G.; GAISER, T.; EWERT, F. Climate change impact under alternate realizations of climate scenarios on maize yield and biomass in Ghana. **Agricultural Systems**, v. 159, p. 157-174, 2018. doi

SPARKS, A.H. nasapower: a NASA POWER global meteorology, surface solar energy and climatology data client for R. **Journal of Open Source Software**, v. 3, 01035, 2018. doi

STRAFFELINI, E.; TAROLLI, P. Climate change-induced aridity is affecting agriculture in Northeast Italy. **Agricultural Systems**, v. 208, 103647, 2023. doi

TAMAKI, T.; NOZAWA, W.; MANAGI, S. Evaluation of the ocean ecosystem: climate change modelling with backstop technologies. **Applied Energy**, v. 205, n. 1, p. 428-439, 2017. doi

TATLI, H. Classification of the Köppen and Holdridge life zones with respect to the climate scenarios-Rcp 4.5 over Turkey. In: **8th Atmospheric Sciences Symposium**, Istanbul, p. 651-657, 2017.

TAVARES, P.D.S.; GIAROLLA, A.; CHOU, S.C.; SILVA, A.J.D.P.; LYRA, A.D.A. Climate change impact on the potential yield of Arabica coffee in southeast Brazil. **Regional Environmental Change**, v. 18, n. 1, p. 873-883, 2018. doi

TAYLOR, K.E.; STOUFFER, R.J.; MEEHL, G.A. An overview of CMIP5 and the experiment design. **Bulletin of the American Meteorological Society**, v. 93, n. 4, p. 485-498, 2012. doi

TEEGAVARAPU, R.S.V.; GOLY, A.; VISWANATHAN, C.; BEHERA, P. Precipitation extremes and climate change: Evaluation using descriptive WMO indices. In: **World Environmental and Water Resources Congress 2012: Crossing Boundaries**, Albuquerque, p. 1927-1936, 2012. doi

TERASSI, P.M.B.; SILVEIRA, H. Aplicação de sistemas de classificação climática para a bacia hidrográfica do rio Pirapó-PR. **Formação (Online)**, v. 1, n. 20, p. 111-128, 2013. doi

THORNTHWAITE, C.; MATHER J. The water balance. **Public. in Climatol.**, v. 8, n. 1, p. 1-104, 1955.

THORNTHWAITE, C.W. An approach toward a rational classification of climate. **Geographical Review**, v. 38, n. 1, p. 55-94, 1948.

TREWARTHA, G.T. **An Introduction to Climate**. New York: McGraw-Hill, 1954.

VAN VUUREN, D.P.; EDMONDS, J.; KAINUMA, M.; RIAHI, K.; THOMSON, A.; *et al.* The representative concentration pathways: An overview. **Climatic Change**, v. 109, n. 1-2, p. 5, 2011. doi

WAISMAN, H.; CONINCK, H.; ROGELJ, J. Key technological enablers for ambitious climate goals: Insights from the IPCC special report on global warming of 1.5° C. **Environmental Research Letters**, v. 14, n. 11, p. 111001, 2019. doi

WMO. **Guidelines on the Calculation of Climate Normals, WMO n°. 1203**, Geneva: WMO, 2017.

WU, T.; LI, W.; JI, J.; XIN, X.; LI, L.; *et al.* Global carbon budgets simulated by the Beijing climate center climate system model for the last century. **Journal of Geophysical Research: Atmospheres**, v. 118, n. 10, p. 4326-4347, 2013. doi

XIAO-GE, X.; TONG-WEN, W.; JIANG-LONG, L.; ZAI-ZHI, W.; WEI-PING L.; *et al.* How well does BCC_CSM1.1 reproduce the 20th century climate change over China. **Atmospheric and Oceanic Science Letters**, v. 6, n. 1, p. 21-26, 2013. doi

XIN, X.; GAO, F.; WEI, M.; WU, T.; FANG, Y.; *et al.* Decadal prediction skill of BCC CSM1.1 climate model in East Asia. **International Journal of Climatology**, v. 38, n. 2, p. 584-592, 2018. doi

ZEROUAL, A.; ASSANI, A.A.; MEDDI, M.; ALKAMA, R. Assessment of climate change in Algeria from 1951 to 2098 using the Köppen-Geiger climate classification scheme. **Climate Dynamics**, v. 52, n. 1-2, p. 227-243, 2019. doi

ZHANG, M.; GAO, Y. Time of emergence in climate extremes corresponding to Köppen-Geiger classification. **Weather and Climate Extremes**, v. 41, 100593, 2023. doi